JOURNAL OF GEOPHYSICAL RESEARCH, VOL. 104, NO. D23, PAGES 30,525–30,557, DECEMBER 20, 1999

A numerical simulation of the stratospheric ozone quasi-biennial oscillation using a comprehensive general circulation model

Lori Perliski Bruhwiler [1] and Kevin Hamilton

NOAA Geophysical Fluid Dynamics Laboratory, Princeton, New Jersey

Abstract. The Geophysical Fluid Dynamics Laboratory's SKYHI general circulation model (GCM) including a new detailed stratospheric photochemistry module has been integrated for over 14 years with an imposed zonally symmetric momentum source designed to force a realistic quasi-biennial oscillation (QBO) in the tropical stratosphere. The GCM features an internally consistent calculation of the annual stratospheric circulation cycle and exhibits realistic extratropical stratospheric interannual variability, making it appropriate for the detailed investigation of QBO/annual cycle interactions. The simulated ozone QBO is generally realistic in the tropics and subtropics, and, in particular, the QBO in total column ozone agrees quite well with that derived from satellite observations. A detailed analysis of the QBO modulation of the zonal-mean ozone budget has been performed. The advective effects of the QBO-induced residual mean circulation are found to be strongly dependent on season, in accord with recent results from some two-dimensional model studies [*Jones et al.*, 1998; *Kinnersley and Tung*, 1998]. In addition, the QBO modulation of explicitly resolved eddy transport in the GCM is found to make a significant contribution to the ozone budget, and this helps account for the strong seasonal synchronization of the ozone QBO.

1. Introduction

The stratospheric quasi-biennial oscillation (QBO) is the dominant source of interannual variability in the tropical and subtropical stratosphere [e.g., *Randel et al.*, 1998]. It is also responsible for a significant amount of interannual variability at high latitudes [e.g., *Holton and Tan*, 1980; *Baldwin and Tung*, 1994]. Poleward transport of trace constituents from tropical photochemical or tropospheric source regions may be significantly modulated by the phase of the QBO. Thus it is of considerable importance to understand the QBO and its role in determining the global distribution of trace species. Understanding sources of natural atmospheric variability is essential for prediction of anthropogenic influences on global budgets of important atmospheric constituents.

The stratospheric QBO is manifested most obviously as an oscillation in zonal-mean tropical wind between westerlies and easterlies. The basic properties of the wind oscillation have been extensively documented over the past several decades (early references include *Reed et al.* [1961], *Veryard and Ebdon* [1961], and *Angell and Korshover* [1964]; more recent observations are summarized by *Naujokat* [1986] and *Hamilton* [1998b]). The fundamental characteristics of the QBO in the tropical stratospheric mean wind are a 22-34 month period (with an average period of about 27-28 months), and downward propagation of the wind reversals at a rate of about 1-2 km/month. The peak-to-peak amplitude of the oscillation approaches 50 m/s at the equator near 30 hPa, and at most levels the easterly extreme is somewhat stronger than the westerly extreme. The amplitude of the QBO in zonal wind drops off with latitude and has a half-width of about 12°. The QBO amplitude drops rapidly below about 50 hPa and is very small near the tropopause ($\sim$ 100 hPa). The current view is that the QBO in the mean circulation is forced largely by the interactions with vertically propagating waves generated in the troposphere [e.g., *Lindzen and Holton*, 1968; *Holton and Lindzen*, 1972; *Dunkerton*, 1997].

Evidence for an extratropical QBO was discussed by *Angell and Korshover* [1964] and later by *Holton and Tan* [1980, 1982]. *Holton and Tan* [1980] used a 16-year data set to document a QBO-related oscillation of zonally averaged geopotential in the Northern Hemisphere (NH) winter stratosphere. In particular, Holton and Tan found that during the westerly (easterly) equatorial phase a positive (negative) midlatitude height

[1] Now at NOAA Climate Monitoring and Diagnostics Laboratory, Boulder, Colorado.

This paper is not subject to U.S. copyright. Published in 1999 by the American Geophysical Union.

Paper number 1999JD900385.

anomaly occurs along with a negative (positive) polar height anomaly. They also found that the amplitude of planetary wave 1 in the high-latitude stratosphere is generally larger during the easterly phase of the tropical QBO. In a later paper, *Holton and Tan* [1982] suggested that the latitudinal displacement of the zonal wind critical surface for stationary waves associated with opposite phases of the equatorial QBO could affect extratropical stationary wave propagation. For boreal winter at 50 hPa, this critical surface (surface of zero mean wind) is generally found near about 20°N during the easterly phase of the equatorial QBO, while during the westerly phase it is located near 6°S. During the westerly phase of the equatorial QBO, the polar vortex tends to be stronger and is maintained longer into the spring season than during the easterly phase. A correlation of the phase of the tropical QBO with the frequency of stratospheric sudden warmings has also been documented [*Labitzke,* 1982; *Dunkerton et al.,* 1988].

A QBO in equatorial column ozone was observed soon after the discovery of the equatorial zonal wind QBO. *Funk and Garnham* [1962] noted a QBO periodicity in ozone observations at two subtropical stations. *Ramanathan* [1963] subsequently suggested an association of the ozone QBO with the stratospheric zonal wind oscillation. Since these early observations, a number of studies have documented the characteristics of quasi-biennial periodicity in total ozone as observed by ground-based or satellite instruments [e.g., *Angell and Korshover*, 1964; *Tolson*, 1981; *Hilsenrath and Schlesinger*, 1981; *Oltmans and London*, 1982; *Hasebe*, 1983; *Bowman,* 1989; *Hamilton,* 1989]. Recently, there have been several studies of the height and latitude dependence of the QBO in ozone and in other trace constituents using Stratospheric Aerosol and Gas Experiment (SAGE) II and UARS Halogen Occultation Experiment (HALOE) and Cryogenic Limb Array Etalon Spectrometer (CLAES) measurements [e.g. *Randel et al.*, 1998; *Randel and Wu*, 1996; *Chipperfield et al.*, 1994; *O'Sullivan and Dunkerton*, 1997; *Zawodny and McCormick*, 1991]. Even the effect of the QBO on observed volcanic aerosol concentrations has been studied [*Hitchman et al.*, 1994].

A conceptual model of the ozone QBO in the tropics and subtropics was advanced by *Reed* [1964], who noted that there should be a low-latitude mean meridional circulation that is associated with the zonal wind QBO. Zonal-mean zonal winds are close to being in thermal wind balance with the zonal-mean temperatures, even quite close to the equator [e.g., *Reed,* 1962]. The expected QBO in zonal-mean temperature has been observed and has a maximum extreme interannual anomaly of up to ~4°C [e.g., *Randel et al.,* 1999], with the warmest equatorial temperatures coincident with the strongest westerly vertical wind shears [e.g., *Angell and Korshover,* 1964]. The temperature QBO in turn should produce an oscillation in diabatic cooling (and hence mean sinking) in regions of westerly vertical wind shear, and diabatic heating (mean rising) in regions of easterly vertical wind shear. Figure 1 is a schematic illustration of this concept (with the addition of the return meridional circulation poleward of about 15° latitude, see below). *Reed* [1964] expressed his notion in terms of the Eulerian mean meridional circulation, but today it is appreciated that the temperature is actually coupled to the diabatic circulation, which should normally be quite close to the transformed-Eulerian mean (TEM) residual circulation [*Andrews and McIntyre,* 1976] and to the relevant Lagrangian transport circulation [*Plumb and Mahlman,* 1987; *Andrews et al.,* 1987].

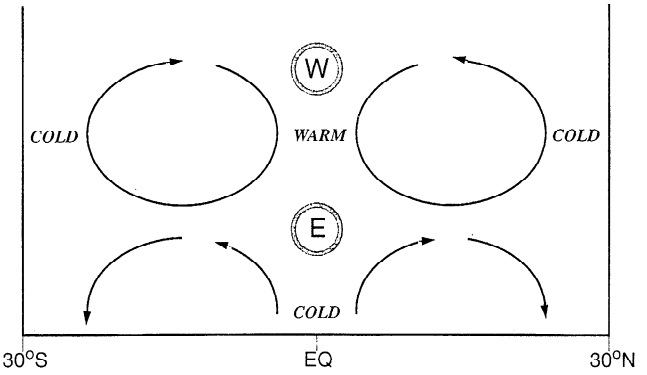

Figure 1. Schematic of the QBO-induced meridional circulation. Descending motion and equatorial outflow occur below the core of the westerly jet, while ascending motion and equatorial inflow occur below the core of the easterly jet.

Reed [1964] proposed that given the vertical stratification of ozone photochemical lifetimes in the stratosphere, the QBO-induced meridional circulation should drive a QBO in total column ozone. When strong equatorial westerlies are present in the lower stratosphere, the atmospheric column has been displaced downward during the descent of the westerly shear zone through the stratosphere. This effectively brings ozone-rich air from its region of maximum photochemical production to the lower stratosphere. Ozone lost at the higher levels is quickly replaced by photochemical production, and the result should be a net increase in total ozone column. When strong easterlies are present in the lower stratosphere, ozone-poor air has been drawn from the lower stratosphere, and the result is a decrease in total ozone column.

Reed [1964] noted that the QBO-related temperature perturbation should change sign at about 15° latitude. Figure 1 illustrates the expected consequence for the QBO mean diabatic circulation: sinking (rising) motion in the tropics should be accompanied by rising (sinking) motion in the subtropics. This would lead in turn to a QBO in total ozone that is out of phase between low latitudes and the subtropics. Observations show that indeed, on average, the column ozone QBO does change phase across ~15° latitude either side of the

equator [*Oltmans and London*, 1982]. In addition, it is also evident from consideration of Figure 1 that the mean horizontal winds associated with the QBO diabatic circulation should converge into (diverge out of) the tropics at levels where there are westerlies (easterlies) on the equator.

The effects of the QBO-induced meridional circulation on ozone at the equator were explored in more detail by *Ling and London* [1986], who used a one-dimensional model with parameterized photochemistry driven by an imposed temperature QBO. Their calculations confirmed the idea that the mean vertical motion associated with the QBO could have an effect on equatorial stratospheric ozone. In particular, the maximum in total column ozone is roughly coincident with peak mean westerlies at 50 hPa, when the atmospheric column has been displaced farthest downward. The calculations of *Ling and London* [1986] also suggested that in the vertical, there are two distinct regions of QBO response in ozone separated by a rather abrupt phase change near 28 km. They attributed the maximum amplitude region near 22 km to transport processes, while the maximum amplitude region near 32 km in their model is due to the local response of temperature-dependent photochemistry to the QBO in temperature. The Ling and London calculations did not include a treatment of NO_x transport, using instead prescribed NO_x values. *Chipperfield et al.* [1994] later pointed out that when this approximation is relaxed, the upper QBO region is actually found to be more strongly related to a QBO variation in NO_x vertical transport. *Randel and Wu* [1996] showed that the interannual variations of SAGE II observations of NO_x and ozone at low latitudes were consistent with the picture of *Chipperfield et al.* [1994].

The first two-dimensional simulations of the ozone QBO that included a detailed photochemical scheme were by *Gray and Pyle* [1989]. Their model included momentum forcing from parameterized equatorial waves that drove a dynamical QBO. included parameterized wave fluxes in their model. They were able to obtain an equatorially trapped region of QBO ozone response with a latitudinal extent somewhat larger than observed. Subsequent work with the same model by *Chipperfield and Gray* [1992] addressed the response of many important stratospheric trace species to the imposed QBO. They concluded that the QBO of relatively long-lived atmospheric species is due to a QBO in transport of the species itself, while the QBO of shorter-lived species is due to a combination of transport of trace species that determine the abundance of the short-lived species and local response of the temperature-dependent photochemistry.

Two intriguing features of the observed ozone QBO are its interhemispheric asymmetry [*Oltmans and London*, 1982; *Hamilton*, 1989], and its seasonal synchronization [*Hamilton*, 1989, 1995b; *Bowman*, 1989; *Tung and Yang*, 1994a]. The extreme total column maxima and minima associated with the QBO off the equator tend to occur in winter in each hemisphere. This is somewhat surprising in light of the apparent interhemispheric symmetry of the QBO zonal wind distribution near the equator. *Holton* [1989] and *Gray and Dunkerton* [1990] argued that the hemispheric asymmetry in the ozone QBO could be due to advection of tropical ozone anomalies (induced locally by the Reed mechanism) to higher latitudes by the seasonal cross-equatorial mean meridional circulation. *Holton* [1989], *Gray and Dunkerton* [1990], and *Tung and Yang* [1994b] all employed simple models to show that this mechanism could indeed produce ozone time series exhibiting a degree of synchronization of the annual and QBO cycles. *Hamilton* [1989], on the other hand, proposed that the QBO modulation of the midlatitude wave guide for stationary planetary waves could be important in explaining the coupling of annual and QBO cycles in ozone. Consider, for example, the case in NH winter. At levels where the tropical mean winds are strongly easterly, the surface of zero mean wind in the NH is located well off the equator, and this surface is thought to act as an effective barrier for equatorward propagation of stationary waves. By contrast, the presence of mean westerlies on the equator may allow planetary waves from the NH to reach very low latitudes and even cross into the Southern Hemisphere (SH). To the extent that dissipating planetary waves act to irreversibly mix chemical constituents, this mechanism would produce a contribution to the ozone budget in the tropics and subtropics that is modulated by both the annual cycle and the QBO. Such a mechanism could also possibly explain the interhemispheric asymmetry of the QBO, since stationary planetary waves are much stronger in the NH than in the SH.

The issue of seasonal synchronization of the QBO has been revisited recently in studies employing zonally symmetric models forced with a QBO-varying momentum source in the tropics. *Jones et al.* [1998; also An analysis of the mechanisms for the quasi-biennial oscillation in ozone in the tropical and subtropical lower stratosphere, submitted to *Journal of Geophysical Research*, 1999 (hereinafter Jones et al., submitted manuscript, 1999)], *Kinnersley and Tung* [1998], and *Kinnersley* [1999] have noted that in their models the QBO-related mean meridional circulation at low latitudes is strongly asymmetric in the solsticial seasons, being much stronger in the winter hemisphere. This produces an annual coupling of the QBO in ozone which resembles that seen in data. These recent studies have also suggested that another aspect of the *Reed* [1964] picture of the ozone QBO needs to be modified. In particular, *Politowicz and Hitchman* [1997], *Jones et al.* [1998; also submitted manuscript, 1999], and *Kinnersley and Tung* [1998] all have found that horizontal advection of ozone by the mean meridional circulation can be as important in the generation of the QBO as the vertical advection invoked by *Reed* [1964].

Most theoretical studies of the effects of the tropical QBO on trace constituents have employed models with zonal-average treatments of atmospheric transport processes. Although this strategy has led to considerable insight into the effects of the QBO on trace species such as ozone, a major limitation is that eddy transport processes must be parameterized. In addition, zonal-average models run with annually repeating external forcing will not exhibit significant interannual variability in the circulation. The research described in the present paper was motivated by the expectation that valuable insights could be gained into the nature of the ozone QBO through a three-dimensional general circulation model (GCM) simulation in which all the eddy and mean transports are determined self-consistently. The simulation of the QBO in a dynamical-chemical GCM is also of interest simply as a means of evaluating one reasonably well-defined aspect of the interannual variability in the model. A somewhat related study focused on QBO effects at high latitudes in the Southern Hemisphere was performed by *Butchart and Austin* [1996] using a three-dimensional mechanistic stratospheric model forced by imposed planetary waves at the lower boundary.

At present, most GCMs are not capable of spontaneously generating a tropical QBO. Recently, there has been some progress reported in this problem. Control integrations with the models of *Takahashi* [1996], *Horinouchi and Yoden* [1998], and *Hamilton et al.* [1999] have all produced large-amplitude QBO-like variations in the equatorial zonal-mean zonal winds. In each case some changes from the usual formulation of the model were required to produce the oscillation. In particular, for all three models it was necessary to run at very high vertical resolution. In the model of *Hamilton et al.* [1999] it was additionally necessary to have very fine horizontal resolution, while the models of *Takahashi* [1996] and *Horinouchi and Yoden* [1998] both had unusually small subgrid-scale diffusion coefficients. Note that all these reported oscillations deviate significantly from the observed QBO in terms of period and vertical amplitude structure. Thus none of these models is appropriate for the present study in which the aim was to examine the detailed chemical response to a realistic QBO in the zonal mean dynamical fields. This goal led to the approach adopted here (and discussed in more detail below) of incorporating a highly parameterized dynamical QBO in a moderate resolution version of a stratospheric dynamical-chemical GCM. This contrasts with the recent study of *Nagashima et al.* [1998], who incorporated a highly parametrized ozone chemistry into the dynamical model of *Takahashi* [1996]. They found that the spontaneous QBO-like oscillation in their model did indeed generate an ozone oscillation with the same period. However, the unrealistic aspects of their dynamical oscillation did not allow a detailed comparison with the observed ozone QBO.

A detailed study of the response of the Geophysical Fluid Dynamics Laboratory (GFDL) "SKYHI" troposphere-stratosphere-mesosphere GCM to an artificially imposed tropical QBO was conducted by *Hamilton* [1998a]. In particular, he added a zonally symmetric QBO zonal momentum source in the tropical middle atmosphere to the standard version of the model and performed a 48-year integration. Detailed analysis of the simulated interannual variability showed that the phase of the tropical QBO significantly affects the frequency of sudden stratospheric warmings, as well as the winter-mean strength of the NH stratospheric vortex. Thus the inclusion of the QBO forcing in the model resulted in an improved representation of the stratospheric interannual variability in both the tropics and extratropics. In the present study, the work of *Hamilton* [1998a] is extended to include a detailed treatment of ozone photochemistry, and the internal consistency of the GCM is exploited to provide a detailed picture of how the QBO affects the interannual variability of stratospheric ozone.

Descriptions of the GFDL SKYHI GCM and the stratospheric photochemical scheme used to calculate ozone are given in the next section, along with a description of the QBO experiment. In section 3 the results for the simulated total ozone QBO are presented and evaluated against satellite observations. The vertical structure of the QBO in ozone and related constituents is discussed in section 4, with an emphasis on determining the photochemical processes that are important for driving the ozone QBO at various altitudes. Section 5 is a detailed consideration of QBO transport effects on the zonal-mean ozone budget. Conclusions and a summary are given in section 6.

2. Model Description

This section begins with a brief discussion of the SKYHI GCM and a description of the implementation of the QBO forcing. The stratospheric photochemical scheme developed for use in SKYHI is then described, as well as the details of the present QBO integration.

2.1. Dynamical Model

The dynamical model used is for practical purposes identical to that described by *Hamilton* [1998a]. This is the SKYHI troposphere-stratosphere-mesosphere GCM [*Fels et al.*, 1980; *Hamilton et al.*, 1995; *Hamilton*, 1995a] run at 3°x3.6° latitude-longitude resolution and with 40 levels between the ground and 0.0096 hPa (~80 km altitude). The model is a fully consistent GCM with realistic topography, a sophisticated radiative transfer calculation, parameterized interactions of the atmosphere with the land/ocean/ice surface, parameterizations of convection, evaporation, precipitation, and subscale diffusive closure. In the experiment considered here (as in the control runs of *Hamilton et al.* [1995],

or the earlier QBO experiment of *Hamilton* [1998a]) the sea surface temperatures are specified to climatological (but seasonally varying) values. Added to the standard version of the model is a zonally symmetric forcing in the zonal momentum equation in the tropical middle atmosphere exactly as described by *Hamilton* [1998a]. In particular, the following term is added at each grid point:

$$\frac{\partial u}{\partial t} = ... - \alpha(\bar{u} - \bar{u_o}) \quad (1)$$

where u is the zonal wind and the overbar indicates the zonal mean. The relaxation rate α is a function of pressure and latitude. On the equator at 28 hPa the relaxation timescale α^{-1} is 5 days. The value of α drops off rapidly in both height and latitude and is zero at pressures higher than 103 hPa (heights roughly below 18 km) and at latitudes greater than 23.5°. The prescribed wind field $\bar{u_o}$ toward which the model is relaxed is a function of pressure, latitude, time of year, and phase of the QBO cycle. It is a sum of the zonal-mean zonal wind in the long-term climatology of the control model and a term designed to force a QBO with realistic vertical and meridional structure. The QBO term is somewhat idealized in being perfectly monochromatic with a period of exactly 2.25 years (about 27 months). Four imposed QBO cycles last exactly 9 years, and so while the relative phase of QBO and annual cycles varies from cycle to cycle, the sequence repeats every 9 years. An important point documented by *Hamilton* [1998a] is that the model responds to the imposed momentum forcing with a QBO in zonal-mean temperature in the tropics and subtropics that is in good agreement with observations.

The addition of the QBO momentum source does little to change the long-term time-mean winds and temperatures of the model, and so the climatology is quite similar to that documented for the 3°x3.6° control model in the works by *Hamilton et al.* [1995] and *Hamilton* [1995a]. While the overall simulation of the large-scale circulation by this model is reasonable, there are some important deficiencies, particularly at high latitudes in the middle atmosphere.

In common with most GCMs, this model produces results in the middle atmosphere characterized by unrealistically weak mean meridional circulation, a temperature structure too close to radiative equilibrium, and middle atmospheric jets that are stronger than observed (see *Hamilton* [1996] for a general review of this issue). The largest temperature biases are near 1 hPa at the winter poles. The simulated temperatures near 1 hPa are lower than observed by as much as 25°C at the North Pole in December-February and lower by more than 60°C at the South Pole in June-August [*Hamilton et al.*, 1995]. These very large temperature biases are largely confined poleward of 60° latitude in each case, and are also less prominent in the lower stratosphere.

The cold temperatures and unrealistically weak circulation in the high latitude winter hemisphere pose a particular problem for the simulation of ozone chemistry, which depends strongly on both local temperature and the large-scale transport. Given the natural focus of the present QBO experiment on relatively low latitudes, it was decided that this version of the dynamical model could be usefully employed. However, the deficiencies in dynamical simulation noted here need to be borne in mind when considering the results. In the discussion of the chemical results, attention will be largely restricted to the region equatorward of about 45°.

2.2. Photochemical Calculation

The photochemical scheme developed for use in SKYHI treats the detailed interactions of reactive oxygen, hydrogen, and nitrogen species. The "family" formalism [e.g., *Garcia and Solomon,* 1983; *Brasseur and Solomon,* 1986] is used to integrate the stiff set of coupled photochemical differential equations forward in time concurrently with the integration of the atmospheric equations of motion. In general, relatively stable chemical species are integrated using some form of numerical differencing (e.g., explicit or semi-implicit), while short-lived species with photochemical lifetimes comparable to or smaller than the model integration time step are diagnosed using either equilibrium or partitioning expressions. In the case of such short-lived species, the chemical tendency greatly exceeds the transport tendency and therefore these species are not transported. Table 1 lists the chemical species categorized according to whether or not they are transported. Fully prognostic (transported) and diagnostic species are shown along with a third category, semiprognostic. This latter category consists of species for which the chemical lifetime may be long compared to the integration time step, but for which the chemical tendency is still much faster than typical transport tendencies. These species may be integrated forward in time as well as diagnosed depending on their chemical lifetimes. It is important to note that many species are long-lived during night, but very short-lived during daylight hours. The scheme is flexible enough to allow for transitions from diagnostic to prognostic solution techniques as warranted, thereby allowing for accurate resolution of the diurnal cycle if desired. Tests have shown that the photochemical scheme remains stable and accurate for time steps up to 30 min. In the present study, the photochemical time step has been chosen to equal the dynamical time step (180 s). At each time step, mass conservation is checked as an indicator of the accuracy of the calculations.

About 60 photochemical reactions are currently included in the scheme. Kinetic data used in the calculation of reaction rates are taken from *DeMore et al.* [1992]. Most of the reaction rates are exponen-

Table 1. Photochemical Species Included in the SKYHI Model

Prognostic	Semiprognostic	Diagnostic
O_x	HO_x	$O(^1D)$,O,O_3 (=O_x)
NO_x	CH_2O	N,NO,NO_2 (=NO_x)
N_2O_5	CH_3O_2	H,OH,HO_2 (=HO_x)
HNO_4	CH_3OOH	
HNO_3		
H_2O_2		
H_2O		
CO		
NO_3		

tially temperature-dependent, and these are precalculated and stored in tables as a function of temperature for computational efficiency. For several reactions, including third-body reactions involving the formation of N_2O_5 and HNO_4, the reaction rate calculation is done on-line due to extremely sharp variation with temperature.

Owing to the large computational expense of calculating photolysis rates in the GCM itself, look-up tables of photolysis frequencies were generated using the quasi-spherical matrix inversion radiative transfer model of *Anderson* [1983]. Absorption cross sections and quantum yields were taken from *DeMore et al.* [1992], while the Schumann Runge band parameterization of *Minschwaner et al.* [1992] was used to calculate O_2 absorption and photolysis. The photolysis rates were tabulated as a function of zenith angle only for simplicity. A more realistic treatment would allow for dependence on temperature, aerosols, clouds, and overhead ozone abundance. Neglect of photolysis rate dependence on temperature is likely to introduce generally small errors into the global photochemical calculation. Aerosols and clouds are very difficult to account for properly due to their large temporal and spatial variations, and are generally neglected in stratospheric photochemical calculations. On the other hand, ignoring the dependence of photolysis rates on overhead column ozone abundance introduces significant limitations into the photochemical calculation. For example, the production of reactive oxygen by O_2 photolysis will not increase in response to overhead ozone decreases (associated with, for example, the QBO, ozone depletion, or the annual cycle in ozone abundance). The effects of this approximation will be discussed in more detail below.

The photochemical scheme used in this study does not include a treatment of halogen chemistry. Halogens were omitted initially for reasons of computational efficiency, although a more current version of the model (not used for this study) does have a detailed treatment of chlorine and bromine chemistry. The chemical loss rate of ozone due to chlorine is about a third of that due to reactive nitrogen in the tropical midstratosphere [e.g., *Perliski et al.*, 1989]; therefore the results presented here should still be fairly representative. Indeed, as will be shown below, the truncated photochemical scheme used in this study still allows for a calculation of the ozone QBO that is fairly representative when compared to observations. The implications of neglecting halogen photochemistry will be discussed further in section 4.

The photochemical calculation was initialized in SKYHI using two-dimensional photochemical model calculations (S. Solomon, personal communication, 1992) and the CIRA O_3 climatology [*Keating et al.*, 1990]. In order to minimize the effects of long-term adjustment to initial conditions, very stable species such as N_2O, CH_4 and H_2 were initialized by scaling to zonally averaged values of N_2O from a multi-decadal SKYHI simulation in which the N_2O should have come close to equilibration.

An important motivation for including detailed photochemical calculations in a GCM is to allow radiative feedbacks between the model dynamics and photochemistry. While this is a long-term goal of the SKYHI model development work at GFDL, the present study was conducted without allowing for these feedbacks. The primary reason for this is that the version of SKYHI used for this study does not have a gravity wave drag parameterization, and therefore the temperatures simulated by the model are often unrealistic enough to significantly degrade the results of the photochemical calculation, especially in the high latitude upper stratosphere. The implications of noninteractive photochemistry for the simulated ozone QBO will be discussed in more detail in the sections below.

Figure 2 shows latitude-season cross sections of column ozone climatology determined from 14 years of Nimbus 7 Total Ozone Mapping Spectrometer (TOMS) observations and from 14 years of the present SKYHI QBO experiment. The overall total ozone distribution and its seasonal evolution are simulated fairly well by SKYHI. The interhemispheric asymmetry in total ozone abundance is also captured reasonably well by the model, with larger amounts of total ozone present

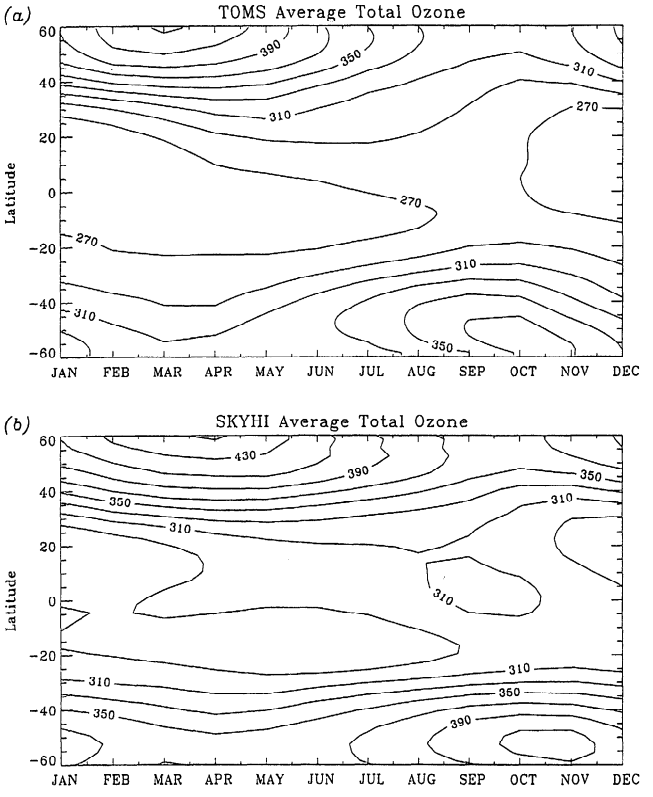

Figure 2. Long-term (14 year) average total ozone calculated for (a) the TOMS observations and (b) the SKYHI calculations (units are in Dobson units (DU) and the contour interval is 20 DU).

in the NH winter than in the SH winter. On the other hand, SKYHI total ozone is systematically high compared to TOMS by 5-12%, with the best comparison in the subtropics and the worst in the polar SH. There are several potential reasons for the discrepancy between the calculated and observed total ozone: neglect of halogen and polar ozone chemistry (of particular importance in the high-latitude austral spring), a simulated meridional circulation that is too weak, and model cold biases. Figure 2 shows, however, that the modeled total ozone bias is fairly consistent over an annual cycle. Therefore its effects on the simulated ozone QBO are likely to be fairly insignificant.

2.3. Experimental Design and Basic Dynamical Results

The photochemical model was run in SKYHI for approximately seven annual cycles without an imposed QBO. March 1 photochemical fields from the end of this run were used as initial conditions for the present QBO experiment, along with dynamical initial conditions obtained for March 1 from a year in the middle of the lengthy QBO experiment of *Hamilton* [1998a]. The dynamical-chemical model was then integrated forward for 17 years. The first three years of this integration are regarded as a "spin-up" period and have been discarded from the analysis. Half-monthly averages (based on 2-hourly snapshots) of important photochemical and dynamical quantities were saved throughout the experiment, including the photochemical and total transport contributions to the time tendency of each constituent concentration. In addition, the model code is set up to compute running averages of the zonal means of quadratic transport terms (e.g., the correlation of meridional wind with ozone concentration around a latitude circle, ozone transport tendencies due to the transformed-Eulerian residual circulation, etc.), again based on 2-hourly sampling. This option was employed only for some selected segments of the integration, notably each of the 14 January and July months in the experiment. These data proved to be very valuable in diagnosing the QBO-related ozone budget (see section 5).

The simulated meridional distributions of anomaly zonal wind, temperature, and meridional wind at the 40 hPa level are shown in Figure 3. Anomaly winds and temperatures were calculated by subtracting from each monthly zonal mean the long-term (14-year average) zonal mean for the same calendar month. For the plot shown in Figure 3 these quantities were further smoothed by Fourier reconstruction excluding periods less than 1 year and greater than 3 years. Throughout this paper the model years are labeled such that the 14-year part of the simulation analyzed extends from January "24" through December "37".

Figure 3a reveals an equatorially symmetric region of alternating westerlies and easterlies largely confined to latitudes between about 20°N and 20°S. The equatorial amplitude of the zonal wind oscillation at this level is over 20 m/s and the associated temperature QBO has an amplitude of 2-3 K, both features in good agreement with with analysis of comparably filtered observations [e.g., *Reed,* 1962, 1964]. In addition, a subtropical temperature QBO that is out of phase with the equatorial temperature QBO is found poleward of about 15° in either hemisphere. The equatorial temperature QBO appears to lag the zonal wind QBO by about 90° so that, for example, the maximum positive temperature anomaly occurs roughly 7 months after the maximum easterly zonal wind. This again is in good agreement with observations [e.g., *Reed,* 1962]. Figure 3c shows that the zonal average anomaly in meridional wind appears basically consistent with the QBO-induced meridional circulation depicted in Figure 1. When there are (westerlies) easterlies at 40hPa, the anomaly zonal average meridional wind displays outflow from (inflow to) the equatorial region.

3. Total Ozone

In this section the simulated zonal-mean column ozone QBO is evaluated against the total ozone QBO seen in 14 complete years (1979-1992) of Nimbus 7 TOMS

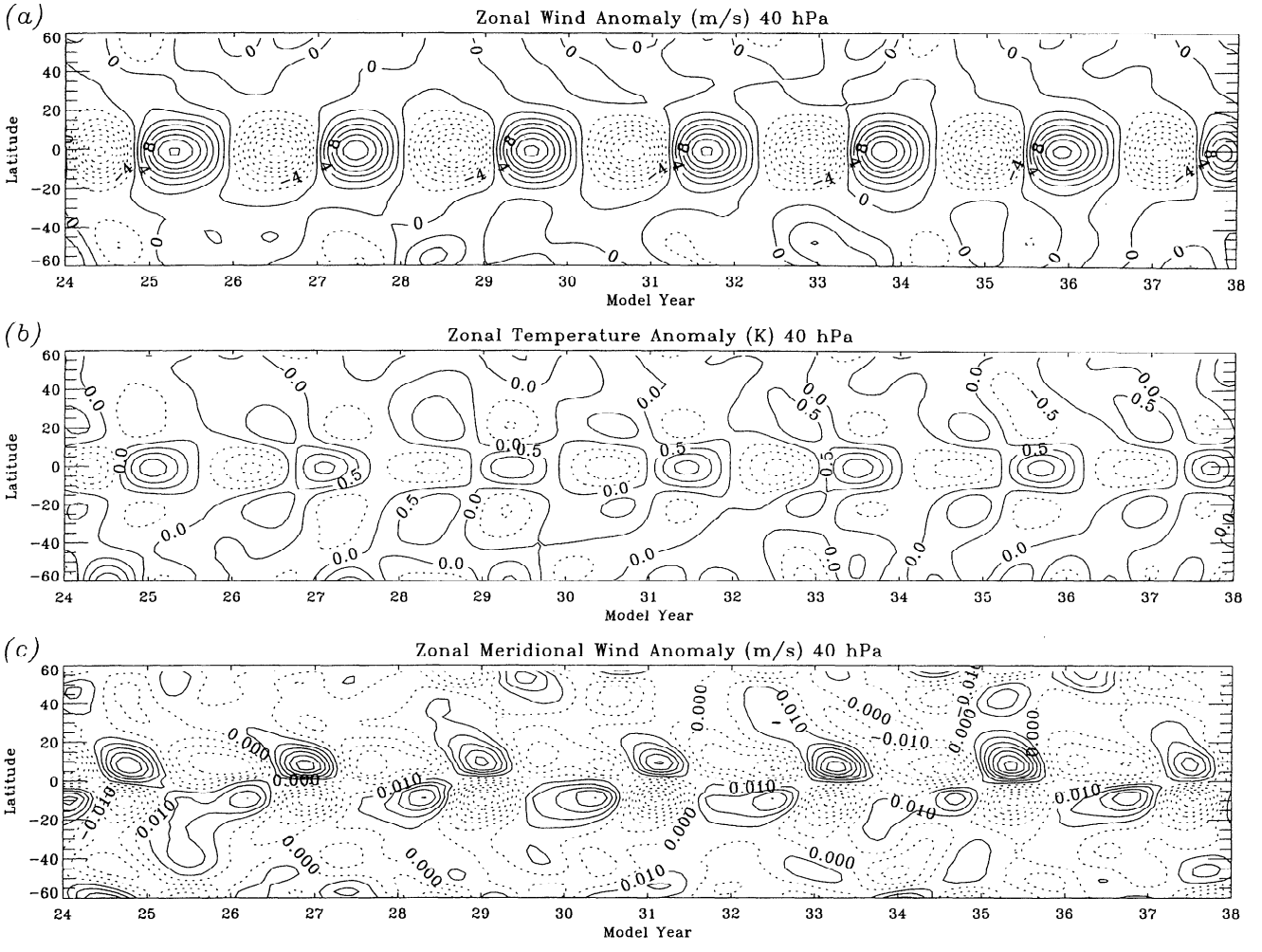

Figure 3. Zonal monthly average anomaly (a) zonal wind, (b) temperature, and (c) (Eulerian) meridional wind at 40 hPa. Units are m/s for the winds and K for temperature. The contour intervals are 2 m/s, 0.5 K, and 0.01 m/s respectively. All quantities shown were filtered in the same manner as the total ozone described in the text.

satellite measurements. Each data set is deseasonalized by subtracting the long-term monthly means. Figure 4 shows slightly smoothed values of the SKYHI total ozone anomaly time series as a function of latitude. The equatorial QBO signal may be discerned clearly in the tropics, but appears to be dominated by higher-frequency variations at higher latitudes. In addition, there is an indication of an increasing total ozone trend, especially in the middle and high latitudes of the NH. It is likely that part of the trend can be attributed to photochemical equilibration from initial conditions. The fields used to initialize the present calculation were obtained from a 2-D model simulation which had a full treatment of halogen chemistry. The photochemical scheme used here, on the other hand, neglects ozone loss by halogens. Therefore the global ozone abundance may be expected to increase, and this adjustment could continue even past the 10 years of spin-up integration that preceded the period shown in Figure 4. On the other hand, there is also an intriguing possibility that at least some of the calculated trend may be related to very long period variations seen in SKYHI dynamical simulations [*Hamilton,* 1995a]. The calculated trend is largest during Northern Hemisphere winter, indicating a possible dynamical role. This simulated long-term ozone trend will be the subject of a future study.

The column ozone anomaly fields for both the TOMS observations and the model simulation, smoothed and detrended by Fourier reconstruction including only periods between 1 and 3 years, are shown in Figure 5. Here the equatorial total ozone QBO is clearly evident, as are the associated subtropical ozone anomalies. The peak-to-peak amplitude of the simulated equatorial column ozone QBO is about 20 Dobson Units (DU), which agrees well with observations. The amplitude of the subtropical column ozone QBO for both the observations and model is comparable to the equatorial amplitude but, on average, it is out of phase (so that a

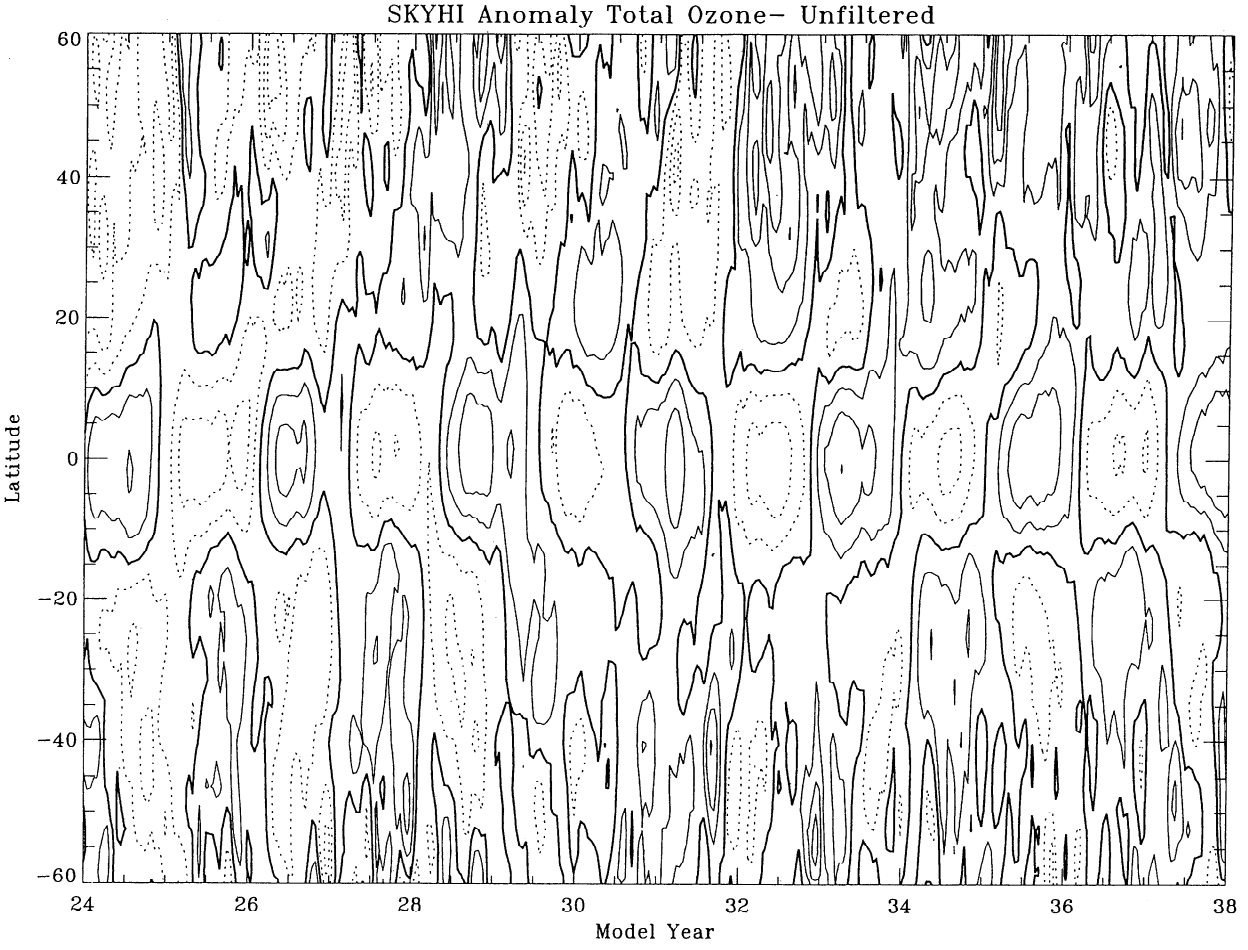

Figure 4. The anomaly in the monthly zonal average SKYHI total ozone (DU). The values plotted were smoothed by calculation of 3-month running means. The thick contour represents the zero contour and the dashed contours indicate negative anomalies. The contour interval is 5 DU.

maximum at the equator is generally coincident with a minimum near 20°). However, inspection of Figure 5 suggests that the QBO in column ozone is not always exactly out of phase between equatorial and subtropical latitudes. Indeed, there is often suggestion of a degree of meridional propagation in both the modeled and observed column ozone anomaly fields (although the appearance of meridional propagation may be dependent on the time filtering employed; a somewhat different analysis of observed total ozone columns by *Randel and Wu* [1996] found little propagation.) In the model simulation the extrema appear first near the equator and then sometimes display poleward propagation in one or both hemispheres. The general pattern is similar, although slightly more irregular, in the observations. A noteworthy feature of the TOMS data is the unusually large negative anomalies appearing at all latitudes during the final year of the record. As pointed out by *Planet et al.* [1994], this has been associated with the eruption of Mount Pinatubo.

Separation of the total ozone anomaly fields into components symmetric and antisymmetric across the equator, as described by *Hamilton* [1995b] can aid in the interpretation of Figure 5. The symmetric component highlights anomalies due to processes which act in phase in both hemispheres. The antisymmetric component, on the other hand, emphasizes processes which are out of phase between the hemispheres, such as the annual cycle and any QBO-annual cycle interactions. Figure 6 shows latitude-time sections of the model-simulated total ozone anomaly for both the symmetric and antisymmetric anomaly components. In comparison to Figure 5b, the symmetric component appears to be much cleaner with less indication of meridional propagation of the QBO total ozone signal. The nodal line, located at about 12° latitude, is also more distinct. The antisymmetric component of the total ozone anomaly tends to be equal to or smaller than the symmetric component in the subtropics, but usually dominates the anomaly at higher latitudes, suggesting the increasing importance of the annual cycle modulation of the QBO.

The latitude dependence of the interaction between the QBO and the annual cycle is further demonstrated by examination of periodograms calculated using the

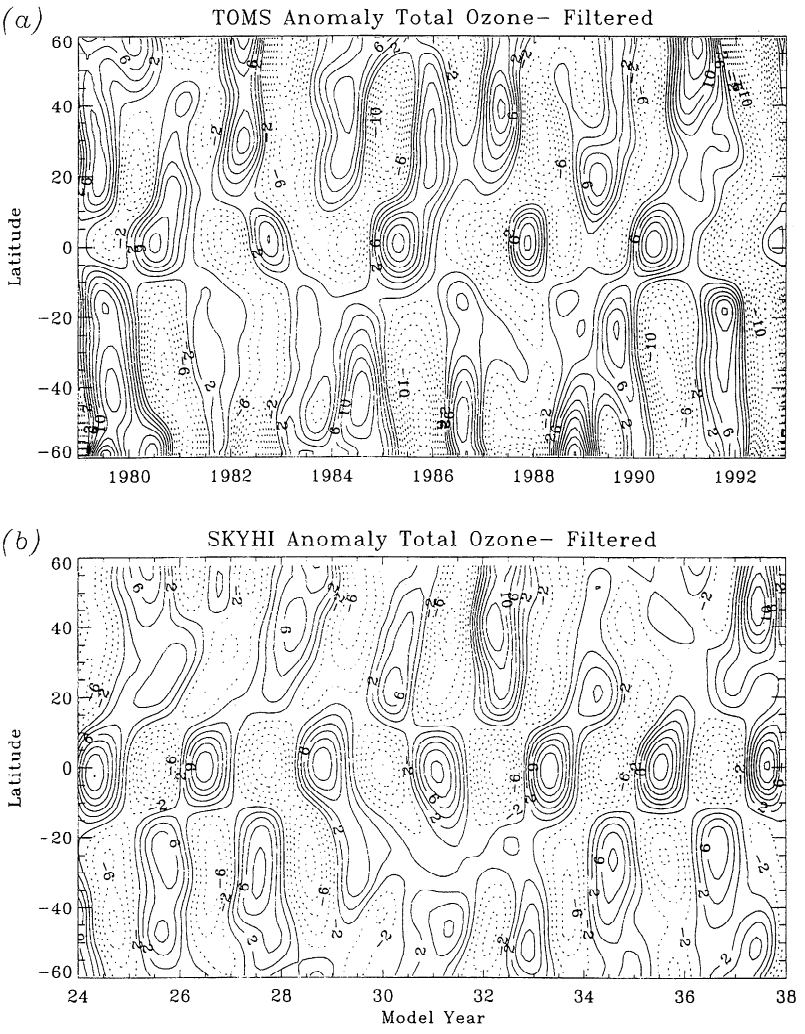

Figure 5. Filtered monthly zonal mean (a) TOMS and (b) SKYHI total ozone anomaly (DU). Observed and modeled total ozone anomalies were filtered as described in the text. The contour interval is 2 DU. Note that for the TOMS data, the time shown on the horizontal axis represents actual years, while for the model calculations the time is in model years. The dashed contours indicate negative ozone anomalies.

modeled and observed total ozone anomaly fields. Figure 7 shows the power for both the model and TOMS at 19.5°N and 19.5°S. Both hemispheres exhibit a strong peak at about 0.43 cycles/yr, which corresponds to the QBO period of 28 months (27 months for the model simulation). A secondary peak at about 0.57 cycles/yr, or a 21-month period, is also evident in both hemispheres, although the simulated peak is considerably weaker than that observed at 19.5°N. The 21-month period corresponds to one of the beat frequencies between the annual cycle and the QBO (i.e., 1/12-1/28=1/21). The other beat frequency is about 1.42 cycles/yr (8.4 months) and is represented by the TOMS observations at 19.5°N. The model seems not to exhibit any clear peak at this higher beat frequency.

At midlatitudes in either hemisphere (Figure 8), the periodograms calculated with TOMS and model ozone anomalies agree less well. At 34.5°N the power at the main QBO frequency in the model results is quite similar to that observed, but the power at the 21-month period is only about one third that seen in the TOMS data. There also appears to be some substantial power at periods less than a year in the observations that is very much smaller in the model (note that the limited sampling of the zonal mean each day in satellite data may act to exaggerate the high-frequency variations in the TOMS time series). At 34.5°S the model very significantly underestimates the power in the main QBO peak, suggesting that simulation of a realistic propagation of the QBO signal to higher latitudes is even more of a problem for the model in the Southern Hemisphere.

4. Vertical Structure of the Ozone QBO

In this section the vertical profile of the ozone response to the imposed QBO is examined in detail. The

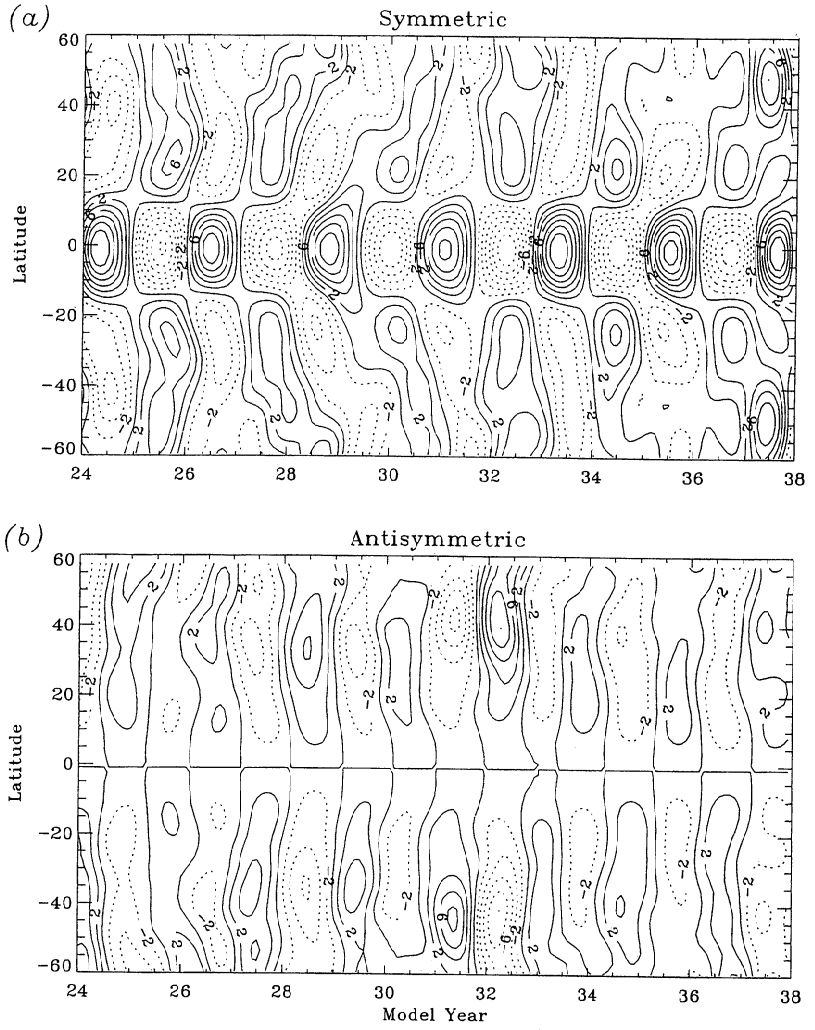

Figure 6. The (a) symmetric and (b) antisymmetric components of the filtered SKYHI total ozone anomalies (DU), calculated as described in the text. The contour interval is 2 DU and the dashed contours indicate negative ozone anomalies.

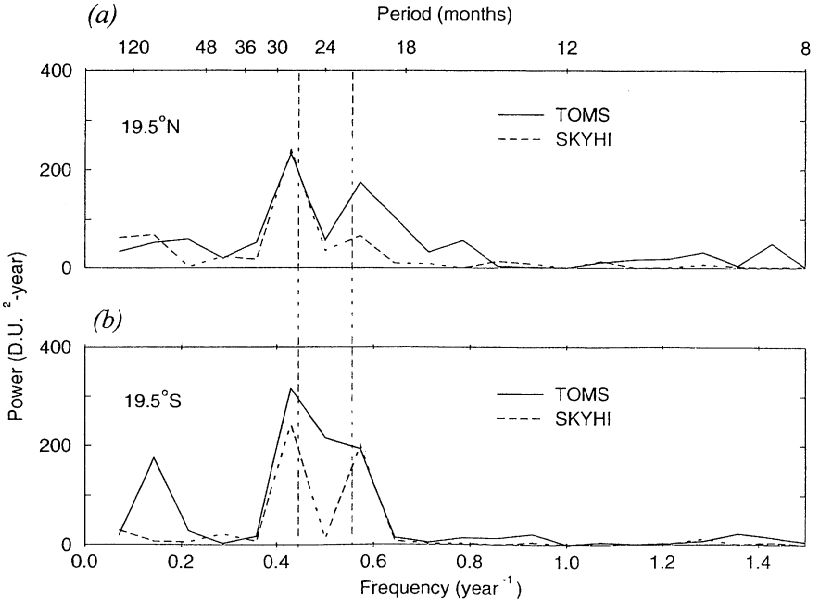

Figure 7. Total ozone anomaly periodograms calculated for TOMS and SKYHI at (a) 19.5°N and (b) 19.5°S. The dashed vertical lines show the frequencies corresponding to the periods of 28 and 21 months.

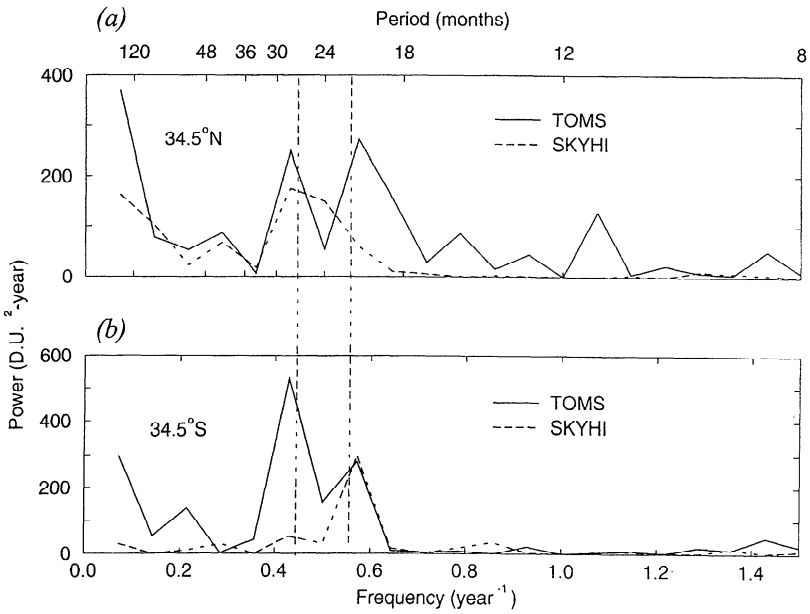

Figure 8. Total ozone anomaly periodograms calculated for TOMS and SKYHI at (a) 34.5°N and (b) 34.5°S. The dashed vertical lines show the frequencies corresponding to the periods of 28 and 21 months.

ozone QBO varies in both phase and amplitude with altitude, and is forced by different processes at different altitudes. The ozone response at a given height also varies significantly with latitude.

4.1. Equator

The height-time evolution of the equatorial zonal-mean zonal wind anomaly is shown in Figure 9a. Once again, the anomaly is defined simply as the deviation from the full 14-year mean for each calendar month, and the anomaly time series have been filtered to retain only periods between 1 and 3 years. Alternating regimes of easterlies and westerlies are seen to propagate downward with a period of 27 months. The transition between easterlies and westerlies is more abrupt than between westerlies and easterlies, in agreement with observations. The magnitude of the maximum zonal wind anomalies exceeds 20 m/s.

The time-height evolution of the equatorial temperature anomaly is shown in Figure 9b. The temperature maxima and minima appear to lag the easterly and westerly jets by approximately 90° and occur in the regions of maximum vertical wind shear. High (low) temperature anomalies occur in regions of westerly (easterly) wind shears. The phase lag and the position of the high and low temperature anomalies are consistent with the QBO-induced meridional circulation described above and illustrated in Figure 1. The maximum amplitude of the temperature QBO is about 2.5°C and occurs near 20 hPa, which is in fairly good agreement with comparably filtered observations [*Reed*, 1962, 1964], although the study by *Randel et al.* [1999] using U.K. Meteorological Office (UKMO) stratospheric analyses suggests that the maximum occurs lower, near 40 hPa.

Figure 9c shows the time-height progression of the simulated equatorial ozone mixing ratio anomalies. It is evident that there are two distinct regions of stratospheric ozone response separated by an abrupt change of phase near 15 hPa. The peak amplitude of the ozone QBO maximum just above 10 hPa is about 0.4 ppmv, while the amplitude in the lower stratosphere, near 30 hPa, is slightly less. These amplitudes represent $\sim 4-7\%$ of the mean values in the middle stratosphere and $\sim 11-12\%$ in the lower stratosphere. While these values are in fairly good agreement with the SAGE II ozone data shown by *Chipperfield et al.* [1994] (see their Figure 1), the amplitude of the ozone QBO in the SKYHI model is slightly smaller than that observed in the midstratosphere and slightly larger than that observed in the lower stratosphere. The underestimation of the midstratospheric ozone QBO amplitude in SKYHI may be due in part to the neglect of halogen chemistry. In their 2-D model study, *Chipperfield and Gray* [1992] obtained a peak-to-peak QBO variation in ClO_y of about 20%, and this acts to enhance the amplitude of their simulated ozone oscillation.

In order to examine the systematic effects of the imposed QBO on the trace constituents, it would be desirable to compare results in the same calendar month, but in exactly opposite phases of the QBO. The design of the present experiment adds a complication to this, however, for the use of a 27-month period means that no two Januaries (for example) have exactly opposite QBO phases. In much of the discussion that follows attention will be concentrated on two consecutive Januaries (model years 33 and 34) which have equatorial wind anomalies that are of opposite sign at most heights, but still do not represent exactly opposite QBO phases.

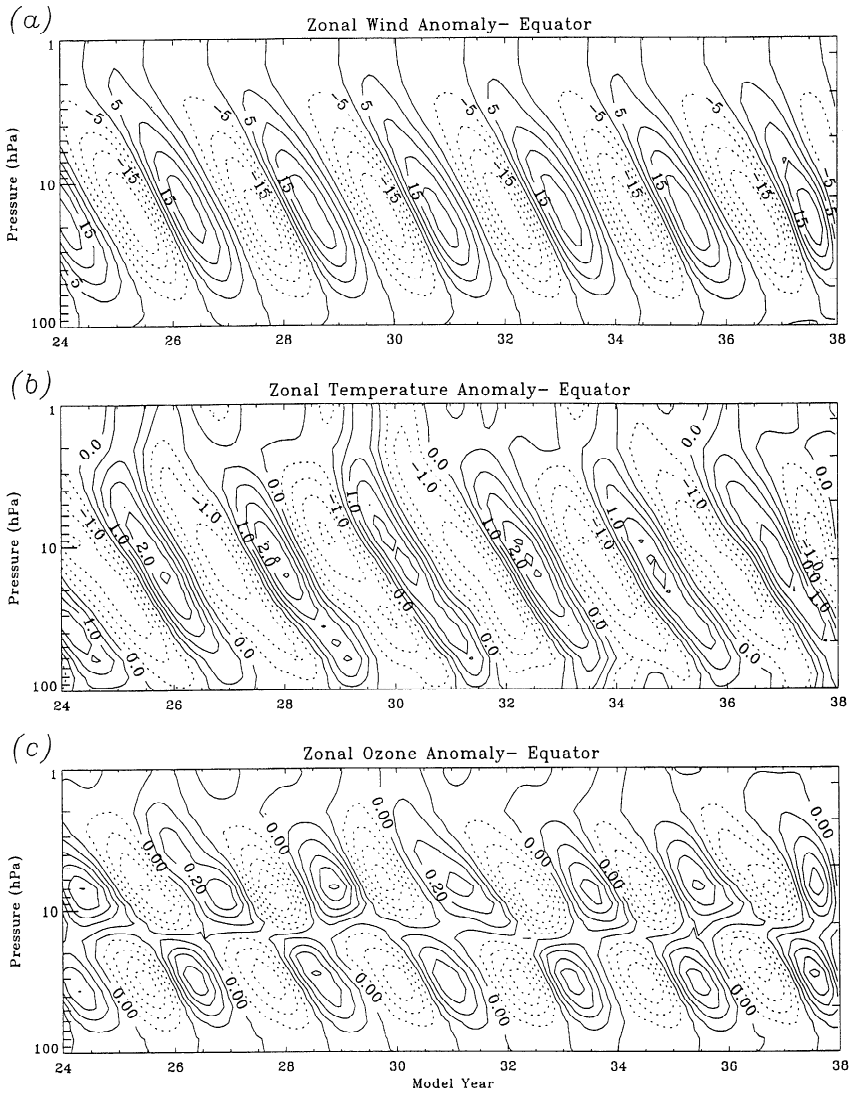

Figure 9. Equatorial (a) zonal-mean anomaly zonal wind, (b) temperature, and (c) ozone. The units are m/s for zonal wind, K for temperature, and ppmv for ozone. The anomaly wind, temperature and ozone were filtered in the same manner as the total ozone. The contour intervals are 5 m/s, 0.5 K, and 0.1 ppmv respectively. Dashed contours indicate negative anomalies.

The zonal-average anomaly photochemical and net transport tendencies at the equator are shown for these two Januaries in Figure 10. The net transport tendency will be decomposed into mean and eddy components below. During January 33 (Figure 10a), the winds between 10 and 20 hPa were strongly westerly. During January 34 (Figure 10b) winds at these levels were strongly easterly. Figure 10 shows that the anomaly ozone response is dominated by QBO-driven changes in the ozone transport tendency below about 10 hPa. In fact, below about 30 hPa the effects of the photochemical ozone tendency are extremely small, as expected. At higher levels the chemical contributions become more significant, so that above about 6 hPa the anomaly chemical tendencies exceed the anomaly transport tendencies for the easterly phase of the QBO shown in Figure 10. For the westerly phase shown in Figure 10, the anomaly chemical and transport tendencies are nearly in balance.

The region between 10 and 6 hPa is interesting, since during the month with westerlies at 15 hPa (Figure 10a) transport effects dominate, while during the month with roughly the opposite QBO phase (Figure 10b), anomaly photochemistry is larger. This is in contrast to previous model studies which have found that QBO-driven photochemical changes are the main cause of the ozone QBO throughout the whole cycle in the region above 10 hPa. Addition of halogen photochemistry to the present model would certainly increase the anomaly photochemical tendencies (perhaps by as much as $\sim 30\%$). Of course, the SKYHI model explicitly simulates the eddy transport, and this may also partly account for differences from earlier 2-D model results.

The anomaly photochemical tendency above 10 hPa

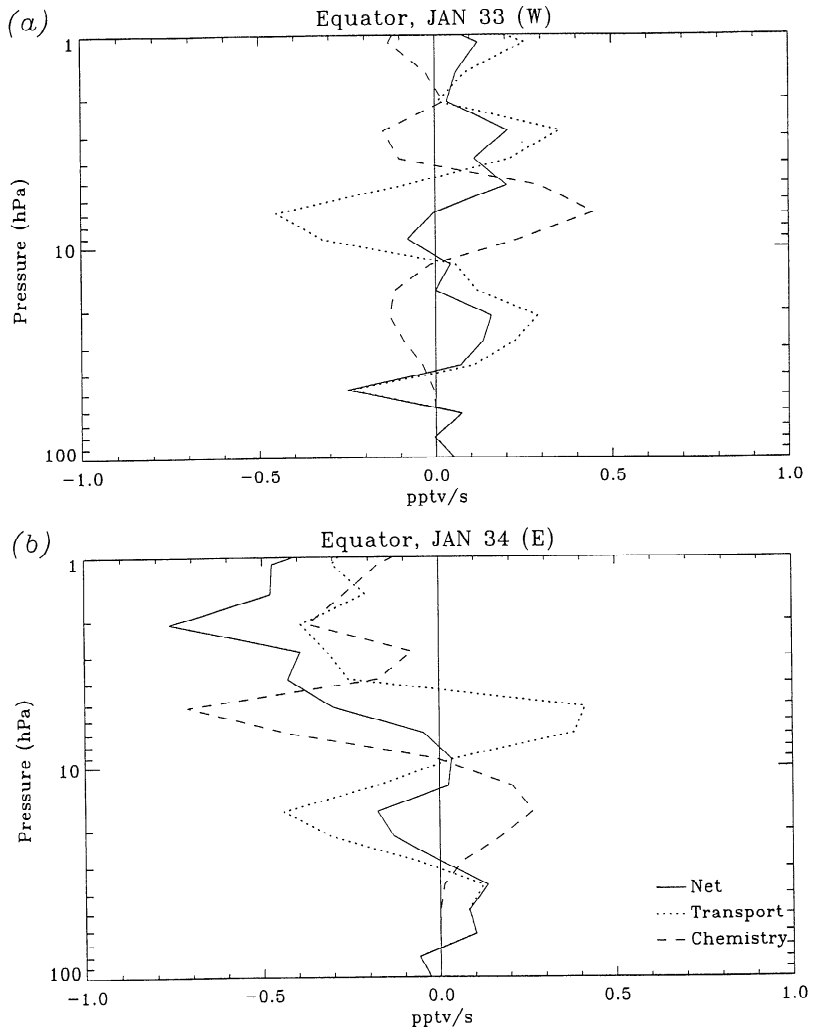

Figure 10. Anomaly net ozone transport and photochemical tendencies for a year during which the phase of the QBO was (a) westerly and (b) easterly. The units are pptv/s.

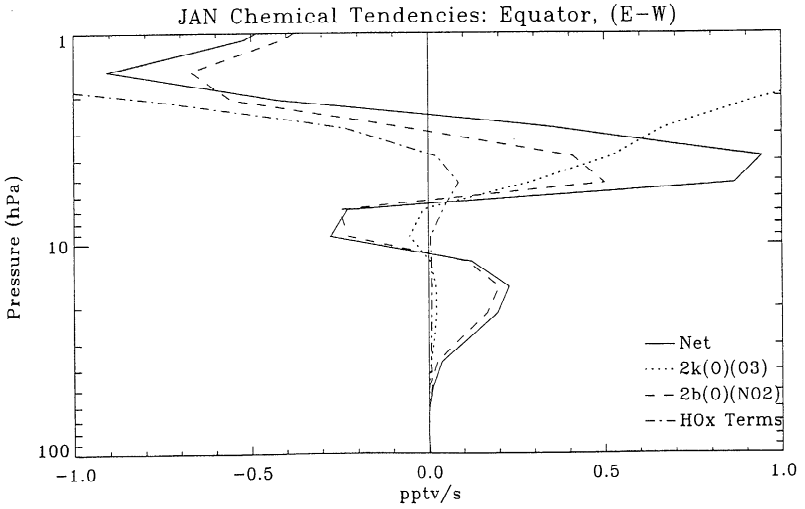

Figure 11. Easterly - westerly phase differences of diurnally averaged ozone loss rates due to NO_x, HO_x, and O_x catalytic cycles. The years differenced were 31 (westerly) and 32 (easterly). The maximum zonal wind anomalies for these years were at approximately the same altitude. Units are pptv/s.

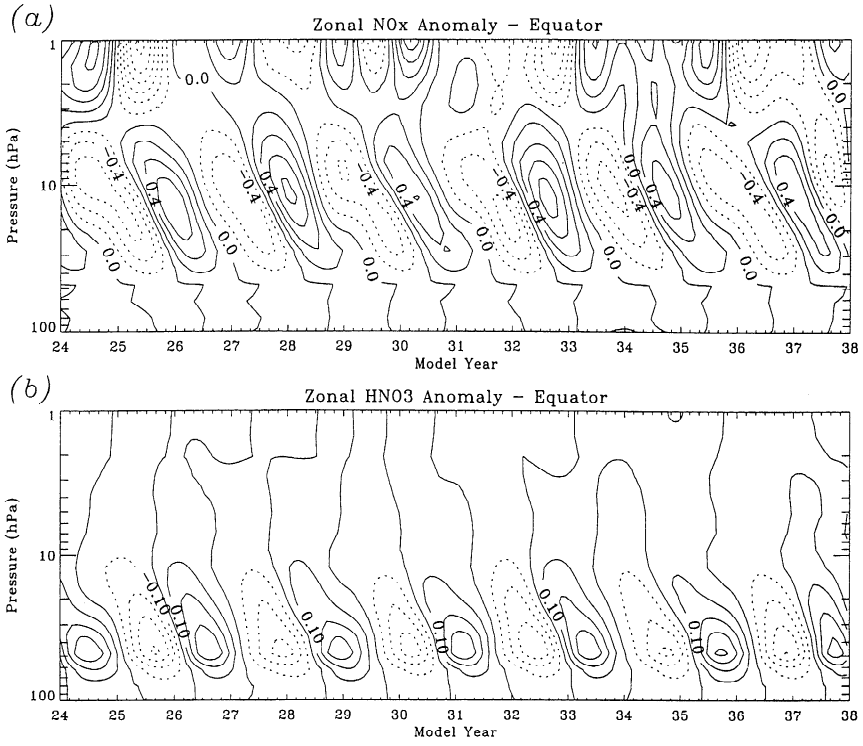

Figure 12. Equatorial zonal-mean anomaly (a) NO_x=NO+NO_2+NO_3+N_2O_5+HNO_4 and (b) HNO_3. Units are ppbv. The NO_x and HNO_3 anomalies were obtained by filtering in the same manner as for total ozone. The contour interval for NO_x is 0.2 ppbv and 0.10 for HNO_3. Dashed contours indicate regions of negative anomalies.

during the westerly phase (Figure 10a) may be interpreted as a decrease in photochemical destruction due to transport of relatively NO_x-poor air from lower levels. Likewise, the negative photochemical anomalies just above 10 hPa in the easterly phase are due to downward transport of NO_x-rich air from the region of calculated NO_x maximum near 3 hPa. Figure 11 is an attempt to show the QBO effects on the chemical tendencies for the rate-limiting steps of the cycles which catalytically destroy ozone. In particular, the difference in the rates in successive Januaries is displayed. For the catalytic ozone cycle involving NO_x the rate-limiting step is the reaction $O + NO_2 \rightarrow NO + O_2$. For odd-oxygen loss, the relevant rate is $O + O_3 \rightarrow 2O_2$. There are several important odd-hydrogen reactions: $H + O_3 \rightarrow OH + O_2$, $OH + O_3 \rightarrow HO_2 + O_2$, $HO_2 + O \rightarrow OH + O_2$, and $OH + O \rightarrow H + O_2$. The sum of these are denoted as "HO_x terms" in Figure 11. The reaction rates k and b for the NO_x and O_x cycles are calculated using the photochemical data of *DeMore et al.* [1992]. See *Perliski et al.* [1989] for a more detailed discussion of the relative importances of different ozone loss rates as a function of altitude and latitude. As shown in Figure 11, below about 6 hPa the easterly phase - westerly phase differences in the photochemical tendency are almost entirely due to changes in the net rate of odd-oxygen destruction by the nitrogen catalytic cycle. This result is consistent with the findings of *Chipperfield et al.* [1994]. Above about 6 hPa the odd-oxygen and hydrogen catalytic ozone destruction cycles become increasingly important.

The time-height evolution of equatorial mixing ratios of NO_x and HNO_3 is shown in Figure 12. Figure 12a shows that the maximum response of NO_x to the imposed QBO occurs in the mid-stratosphere near 10 hPa. The phase of the NO_x variation is such that at times of westerly vertical wind shear, the NO_x anomaly is positive. During times of easterly vertical wind shear, the anomaly in NO_x is at its greatest negative value. This is qualitatively consistent with expected effects of the QBO-induced meridional circulation described previously, since the vertical and poleward gradients of NO_x are positive. The anomaly photochemical and transport tendency profiles for the equatorial NO_x are shown in Figure 13. Near 10 hPa (where the NO_x QBO amplitude is largest) the net anomaly tendency is dominated by transport processes, and anomaly photochemical tendencies are very small, not surprising given the long photochemical lifetimes anticipated for NO_x at these levels [e.g., *Brasseur and Solomon,* 1986; *Chipperfield et al.,* 1994]. At lower levels (say, below 40 hPa) the chemistry becomes significant, consistent with the shorter chemical lifetimes for NO_x in the lower stratosphere [e.g., *Brasseur and Solomon,* 1986]. It is interesting that the anomaly chemical tendencies near 40-50 hPa are so asymmetric between the two Januaries shown, being strongly negative in 33 and much more weakly positive in 34. Comparison with Figure 9c sug-

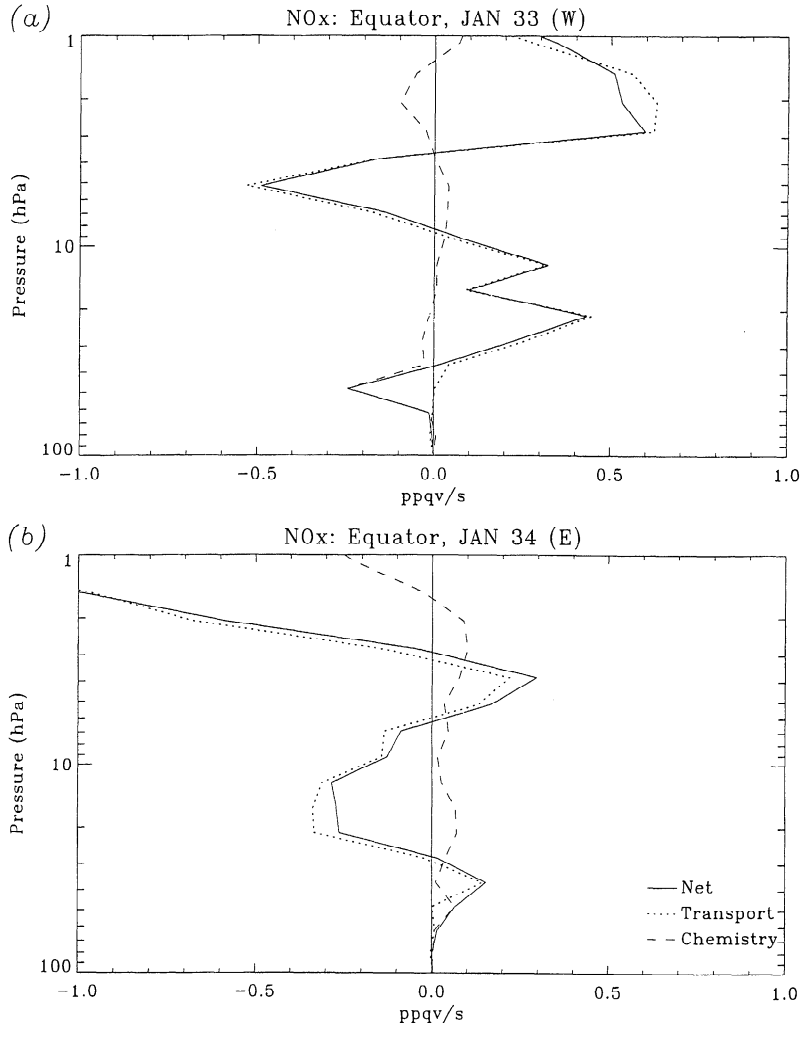

Figure 13. The anomaly net transport and photochemical tendencies for NO_x for a year during which the phase of the QBO was (a) westerly and (b) easterly. Units are ppqv/s (parts per quadrillion by volume per second, or 10^{-6}ppbv/s).

gests that the large negative anomaly in NO_x during the westerly phase is linked to a positive O_3 anomaly near 40 hPa. As discussed by *Chipperfield and Gray* [1992], the positive temperature anomaly associated with the downward QBO-induced circulation during the westerly QBO phase, along with increased transport of ozone to this level shifts the temperature-dependent NO-NO_2 partitioning in favor of NO_2. This leads to more rapid loss of NO_x during the westerly QBO phase due to formation of HNO_3 by reaction with OH. This picture is at least qualitatively consistent with the equatorial NO_x tendencies shown in Figure 13.

The simulated QBO response of HNO_3 (Figure 12b) differs greatly from that exhibited by NO_x. The maximum anomaly occurs in the lower stratosphere, near 40 hPa. The vertical gradient of HNO_3 is negative, while the poleward gradient is positive. Therefore, negative HNO_3 anomalies occur in association with tropical westerly shear and tropical outflow. Likewise, positive HNO_3 anomalies occur when the tropical vertical motion is upward and tropical inflow brings in air that is higher in HNO_3 from midlatitudes. Figure 14 shows the transport and chemical contributions to the equatorial HNO_3 QBO anomaly tendency for January 33 and 34. At most heights the transport and chemical terms have opposite signs, consistent with a chemical timescale (~1 month) considerably shorter than the QBO timescale. During the westerly QBO phase, it is interesting to note that the anomaly photochemical tendency displays a sharp maximum between 40 and 50 hPa. This feature is related to the large anomaly photochemical NO_x loss shown in Figure 13, and is driven by readjustment of the NO/NO_2 ratio in favor of NO_2, which then results in an increase in HNO_3 formation due to the reaction of NO_2 and OH.

4.2. Subtropics

Figure 15 shows the simulated anomaly time series for the zonally averaged zonal wind, temperature, and ozone mixing ratio at 25°N. The zonal wind QBO at

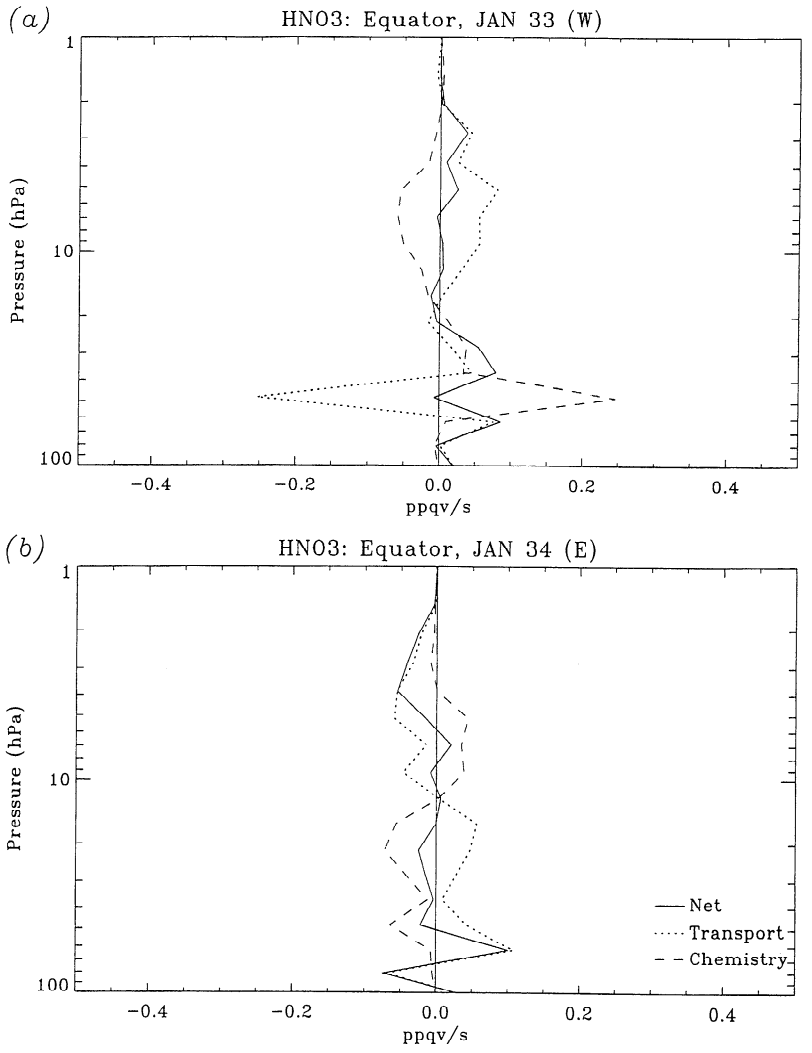

Figure 14. The anomaly net transport and photochemical tendencies for HNO_3 for a year during which the phase of the QBO was (a) westerly and (b) easterly. Units are ppqv/s (parts per quadrillion by volume per second, or 10^{-6}ppbv/s).

this latitude has an amplitude of about 4 m/s (compared to 20 m/s in the tropics). The QBO in temperature is somewhat smaller than that at the equator, but downward- propagating regions of alternating warm and cold anomalies are still quite evident. It is expected that cold subtropical anomalies will be associated with rising motion in the subtropical branch of the QBO-induced meridional circulation (e.g., westerly shear at the equator; see Figure 1). The amplitude of the simulated temperature QBO at 25°N is about 1°-2°C.

The maximum peak-to-peak amplitude of the ozone QBO at 25°N in the SKYHI simulation is about 0.6-0.8 ppmv (Figure 15c), comparable to that at the equator. The subtropical ozone anomaly evolution is characterized by a simple downward propagation without the abrupt phase reversal seen in the equatorial ozone anomalies (Figure 9c). The maximum amplitude in the ozone mixing ratio anomaly QBO at 25°N occurs near 10 hPa. Figure 16a displays the anomaly time series for NO_x at 25°N. At this latitude the NO_x and ozone anomalies are largely anticorrelated (compare Figures 16a and 15c). This would be consistent with the notion of a subtropical ozone QBO that is a photochemical response to the QBO-induced NO_x anomalies. The actual situation seems more complicated, as illustrated in Figure 17 which shows vertical profiles of the anomaly photochemical and transport ozone tendencies at 25°N for two Januaries. Below about 20 hPa the transport tendencies clearly dominate the chemical contribution, while above this height the chemistry is very important.

The time series of NO_x anomaly depicted in Figure 16a is much more complicated than its tropical counterpart (Figure 12a). In particular, some years exhibit two regions of maximum response in the vertical which are out of phase. Other years show only one region of anomaly which tends to be located at somewhat higher

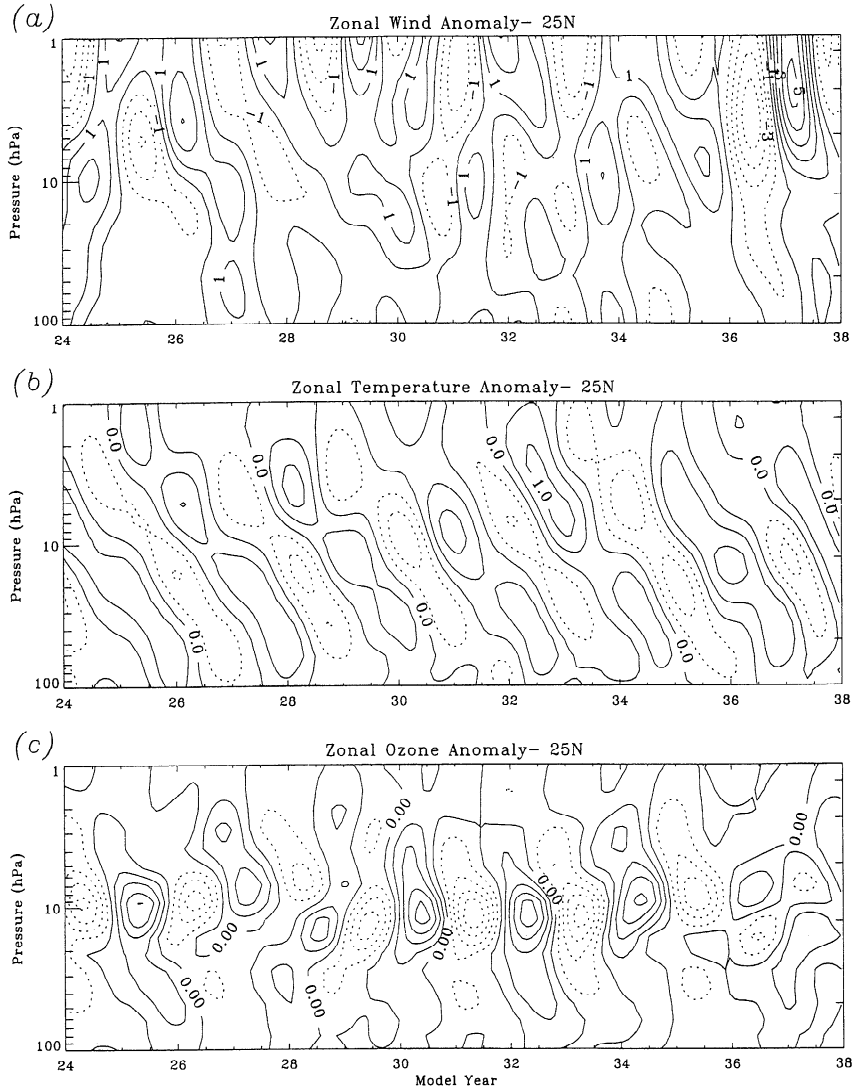

Figure 15. Zonal-mean anomaly (a) zonal wind, (b) temperature, and (c) ozone at 25°N. The units are m/s for zonal wind, K for temperature, and ppmv for ozone. All quantities were filtered in the same fashion as total ozone. The contour intervals are 1 m/s, 0.5 K, and 0.1 ppmv respectively. Dashed contours indicate negative anomalies.

altitude. This picture is, however, consistent with the expected effects of the QBO-induced mean vertical motion. A tropical westerly shear near 40 hPa, for example, should result in horizontal outflow at lower levels, rising motion at 40 hPa in the subtropics, and horizontal flow into the tropics at higher levels. The opposite arrangement should hold for easterly tropical shear. For NO_x, low-level tropical outflow will result in a negative anomaly tendency since the poleward NO_x gradient is positive. Rising subtropical motion also results in negative NO_x anomaly tendencies given the positive NO_x gradient with altitude. The two-cell NO_x anomaly structure progresses upward with time in the model calculation due to the evolution of the QBO-annual cycle phase differences. During model years 29 through 33, the phase of the upper NO_x anomaly maximum shifts by 180°. This is due to the fact that the poleward NO_x gradient in the upper stratosphere becomes negative.

The simulated HNO_3 anomalies at 25°N are shown in Figure 16b. Below about 30 hPa these are generally out of phase with the equatorial HNO_3 anomalies (Figure 12b), consistent with the expected effects of advection by the QBO-induced meridional circulation. However, the picture is more complicated higher up and, in contrast to the equatorial results, the subtropical HNO_3 anomalies often display two regions in the vertical that are opposite in sign. In the lower stratosphere the anomaly is negative during times of tropical outflow (westerly shear near the equator) and positive during tropical inflow (easterly shear near the equator), consistent with the positive poleward HNO_3 gradient.

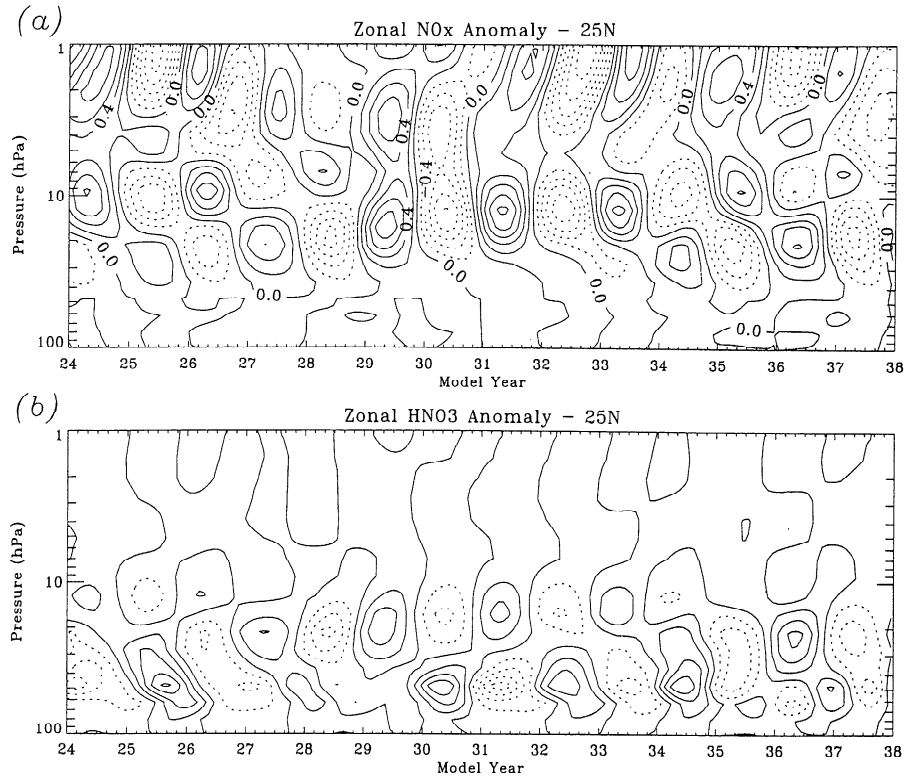

Figure 16. Zonal-mean anomaly (a) NO_x and (b) HNO_3 at 25°N. Units are ppbv. The anomalies were filtered in the same manner as for total ozone. The contour intervals are 0.2 and 0.1 ppbv. Dashed contours indicate negative anomalies.

5. Eddy and Residual Mean Meridional Circulation Contributions to the Transport Tendencies

In the previous section, consecutive Januaries with near-opposite QBO phase were examined to diagnose the causes of the QBO-induced ozone perturbations. Net anomaly transport tendency profiles at the equator are shown for a number of individual Januaries in Figure 18. The years are grouped by the sign of the equatorial zonal mean wind anomaly at 40hPa, with westerly phases in Figure 18a and easterly phases in Figure 18b. It appears that the QBO phase has a fairly consistent and systematic effect on the transport in the model. Note that the curves in each panel are somewhat displaced in the vertical, simply reflecting the range of QBO phases actually occurring in individual Januaries. Note also that the Januaries for which the QBO phase is exactly the same, such as 24 and 33 for example, exhibit variability as well, which must result from internally generated interannual variability of the model circulation. It is noteworthy that the transport tendency curves for years when westerlies were present in the lower stratosphere are more tightly grouped than for years with mean easterlies in the lower stratosphere.

Figure 19 shows the equatorial anomaly transport tendency divided into components due to the transformed Eulerian residual mean circulation, the explicitly resolved eddies, and the parameterized subgrid-scale diffusion terms. Results are shown again for two consecutive Januaries. Figure 20 presents the same quantities at 25°N. Several important conclusions may be reached from inspection of these figures. First, the anomaly transport tendency due to subgrid-scale processes (parameterized as vertical and horizontal diffusion) is generally small compared with either of the other terms. At the equator the contribution from the mean residual circulation is larger at most heights than that from the eddies, but the eddy contribution is still quite significant (up to 50% or more of the mean circulation component at some heights). At 25°N the contribution of the eddy term to the transport tendency is even more significant. The remainder of this section will be devoted to a more detailed investigation of the nature of the mean and eddy contributions to the transport tendency.

Stream functions of the anomaly in the transformed-Eulerian residual circulation are shown together with latitude-pressure cross sections of anomaly ozone for January 31 and 32 (Plate 1). Also shown in the right panels of this plate is the monthly mean zonal-mean equatorial zonal wind for these months. The dashed stream function contours indicate a clockwise circulation, while the solid stream function contours indicate a counterclockwise circulation.

The overall picture of the QBO-induced residual

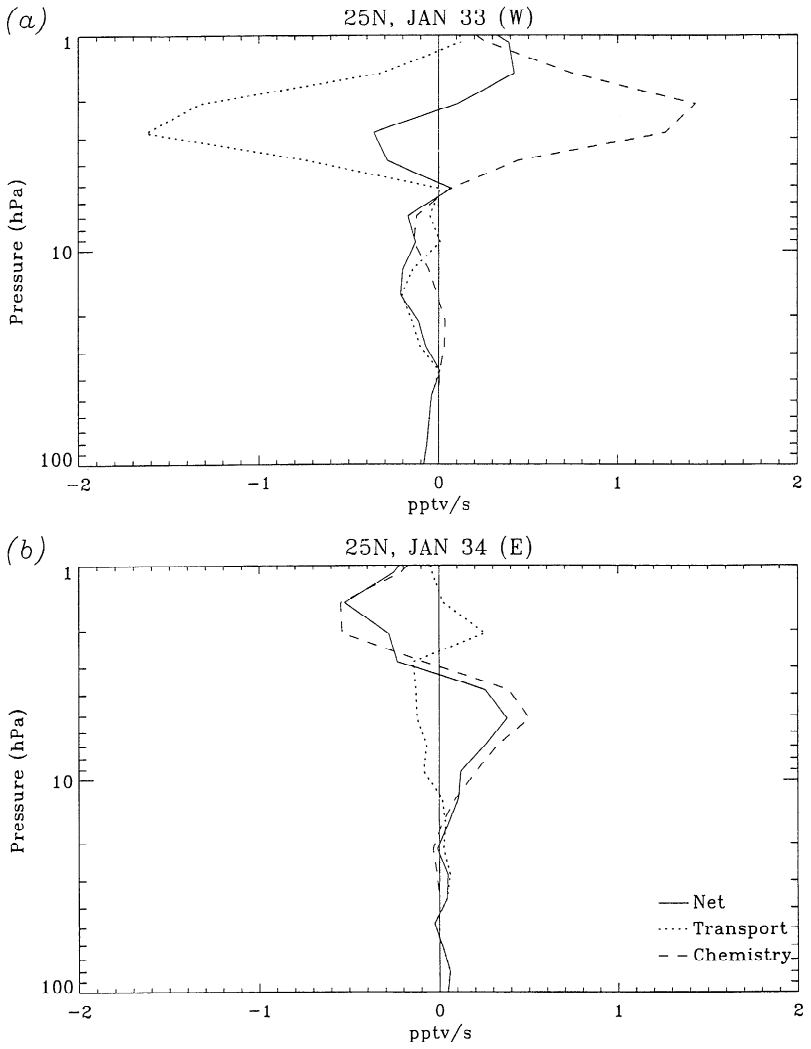

Figure 17. The anomaly net ozone transport and photochemical tendencies for 25°N for a year during which the phase of the QBO was (a) westerly and (b) easterly in the lower stratosphere. The units are pptv/s.

meridional circulation is roughly in accord with the simple scheme illustrated in Figure 1. At the equator there is mean rising motion in westerly shear regions and mean sinking in the easterly shear regions. This leads to horizontal outflow from (inflow to) the equator near the levels of peak equatorial easterlies (westerlies). The main deviation from the simple picture of the residual circulation is the very obvious interhemispheric asymmetry. The QBO-induced residual circulation is much stronger on the winterside of the equator than on the summerside. This is in good agreement with the results from the 2-D models of *Jones et al.* [1998; also submitted manuscript, 1999] and *Kinnersley and Tung* [1998]. In July (not shown) the same effect is apparent in the present SKYHI simulation (i.e., stronger residual circulation in the Southern Hemisphere tropics and subtropics).

The QBO effects on ozone can also be seen quite clearly in Plate 1. For example, the upward motion at the equator associated with the easterly shear above about 20 hPa during January 31 results in lower NO_x just above 10 hPa at the equator, and thus a positive ozone anomaly. In the subtropics the negative ozone anomaly at these heights may be due to downward mean transport of NO_x-rich air.

As previously discussed, the phase of the QBO is expected to strongly influence extratropical planetary wave propagation into the tropics. Plate 2 demonstrates how the mean wind structure modulates the eddy contribution to the ozone transport. This plate shows the zero contour of zonal-mean zonal wind field superimposed on the eddy component of the anomaly ozone transport tendency. Results are presented first for January 31, when the zonal winds are westerly throughout the lower stratosphere and the zero wind line extends to about 15°S between 19 and 70 hPa. In this case a region of negative eddy anomaly transport tendency is apparent between the equator and about 10°N,

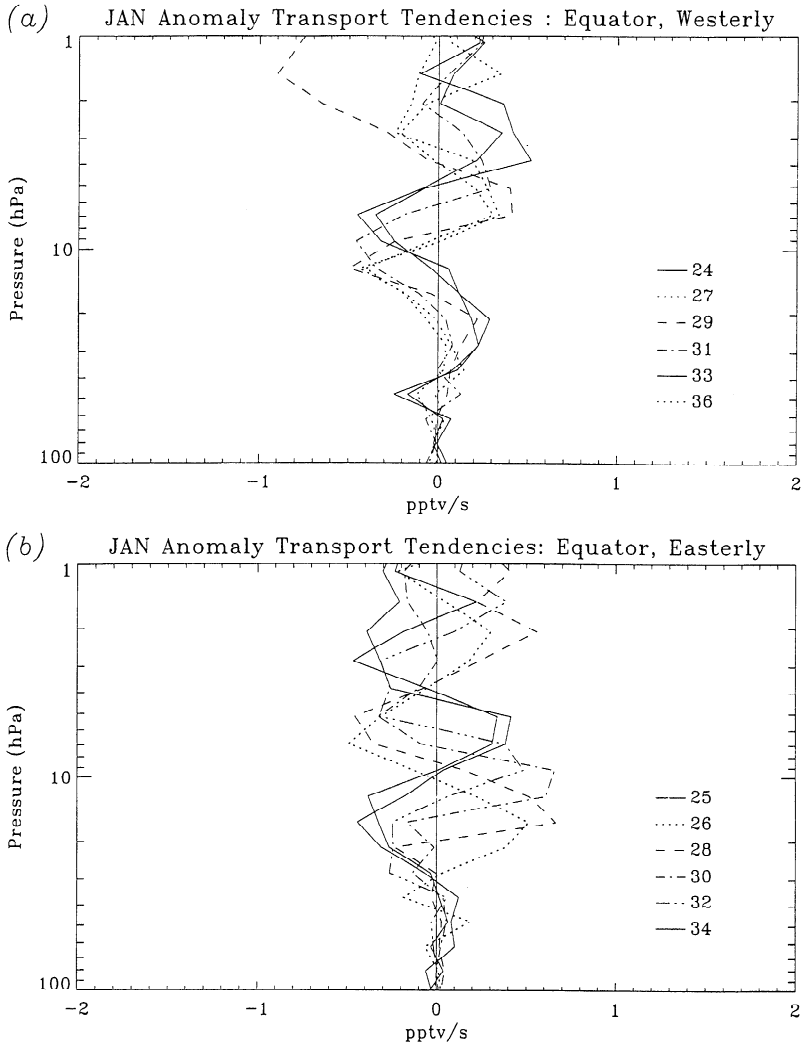

Figure 18. Anomaly ozone tendencies for selected years for which the phase of the QBO in the lower stratosphere was (a) westerly or (b) easterly. Note that years for which the QBO phase was repeated, such as 24 and 33, are plotted with the same type of line.

extending from about 3 hPa to 50 hPa, and a corresponding positive anomaly region is apparent between about 15°N and 30°N. In January 32 the QBO is in nearly the opposite phase, and the zero wind line is located near 30°N. In this month the eddy transport anomaly tendencies have a similar pattern, but the opposite sign as in January 31. This again demonstrates that the QBO modulates the eddy transports in a very systematic fashion. When there are mean westerlies in the equatorial region, the eddies act more efficiently to transport ozone from the equator to higher latitudes, effectively acting as strong horizontal mixing within in the 0°-25°N latitude band. This is consistent with the speculation advanced by *Hamilton* [1989].

Several recent observational studies [*Hasebe,* 1994; *Randel and Wu,* 1996, *Randel et al.,* 1998] have demonstrated that below about 30 hPa there is an approximate in-phase relationship between the QBO signals in ozone and in derived downward vertical velocity (essentially proportional to the local temperature anomaly). This is in contrast to Reed's picture of the QBO in which the ozone anomalies are generated by transport across the vertical ozone gradient, resulting in a maximum ozone anomaly that would be expected to lag the maximum (downward) vertical velocity anomaly by a quarter of a cycle. It has been pointed out by *Politowicz and Hitchman* [1997] and *Jones et al.* [1998; also submitted manuscript, 1999] that horizontal ozone advection could also make an important contribution to the QBO anomalies in trace species. The two-dimensional model calculations of Jones et al. (submitted manuscript, 1999), suggest that the maximum anomalies in the vertical and horizontal transport tendencies are usually of roughly the same magnitude, but almost exactly out of phase.

Time series of equatorial temperature and ozone from the present SKYHI experiment are shown in Figure 21 for several pressure levels. These values have been

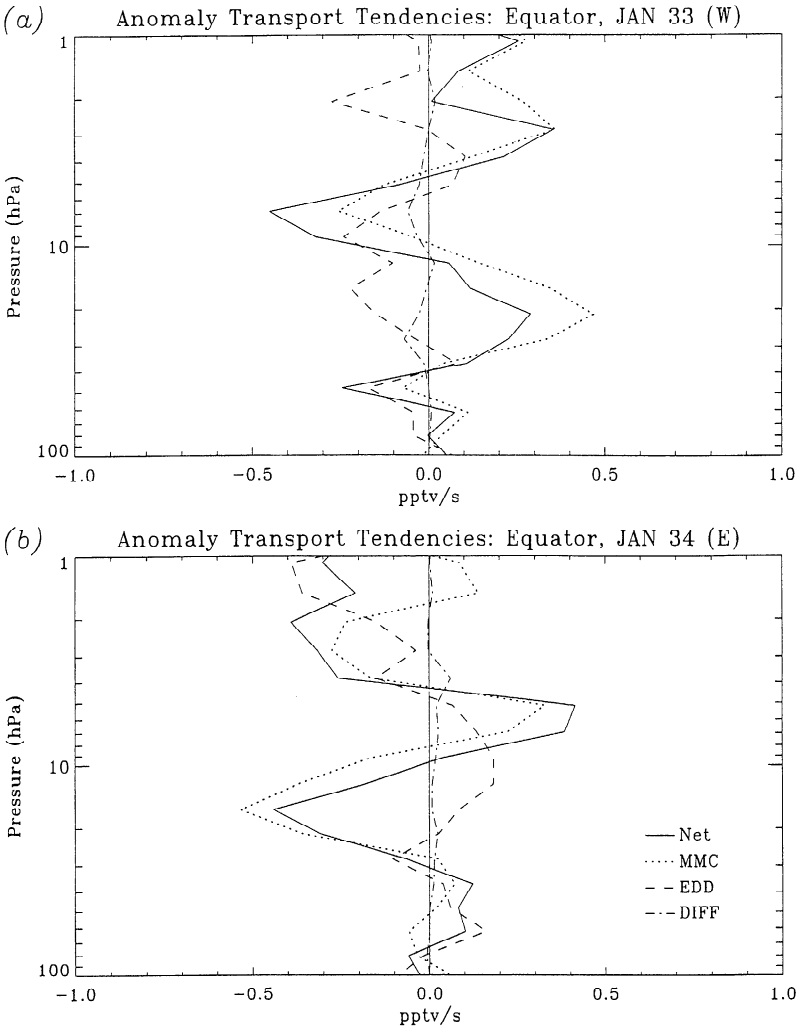

Figure 19. Equatorial anomaly ozone tendencies due to transport by the transformed mean meridional circulation (MMC, dotted line), eddies (EDD, dashed line), and diffusion (DIFF, dashed-dotted line) at the equator for (a) the westerly phase and (b) the easterly phase. Units are in pptv/s. The net transport tendency (NET, solid line) is the sum of the tendencies due to the mean meridional circulation, eddies and diffusion.

Fourier- filtered to retain only periods between 1 and 3 years. Consistent with the observational studies mentioned above, the equatorial ozone and temperature anomalies near 40 hPa are almost exactly in phase, with maximum temperature anomalies tending to slightly lead the maximum ozone anomalies. This agrees well with the observational studies, but it is interesting to note that this in-phase relationship is less evident in the unfiltered monthly mean time series. The time filtering adopted here presumably has a similar effect as the empirical orthogonal function filtering adopted by *Randel et al.* [1998]. Near 20 hPa the maximum ozone anomalies appear to lag the maximum temperature anomalies by about a quarter of a cycle, while at 10 hPa the temperature and ozone QBO anomalies are almost exactly out of phase. As previously discussed, the jump in ozone QBO phase with altitude is due to the influence of a QBO cycle in NO_x transport in the midstratosphere.

Figure 22 shows time series of the total transport tendency for ozone near 40 hPa at the equator and 22.5°N. Since the detailed zonal-mean averages of the quadratic transport terms were archived only in January and July, this figure (and subsequent figures) shows transport terms for only those two months (although the series of zonal-mean zonal wind shown for comparison does include all months). The systematic modulation of the net transport tendency by the QBO is quite evident in both figures, although the behavior of the net transport tendency at 22.5°N is dominated by the annual cycle. At the equator near 40 hPa, local easterlies on average correlate with negative extremes in the net transport tendency, while local westerlies tend to correlate with small or positive net transport tendency. If vertical transport of ozone by the mean circulation were the

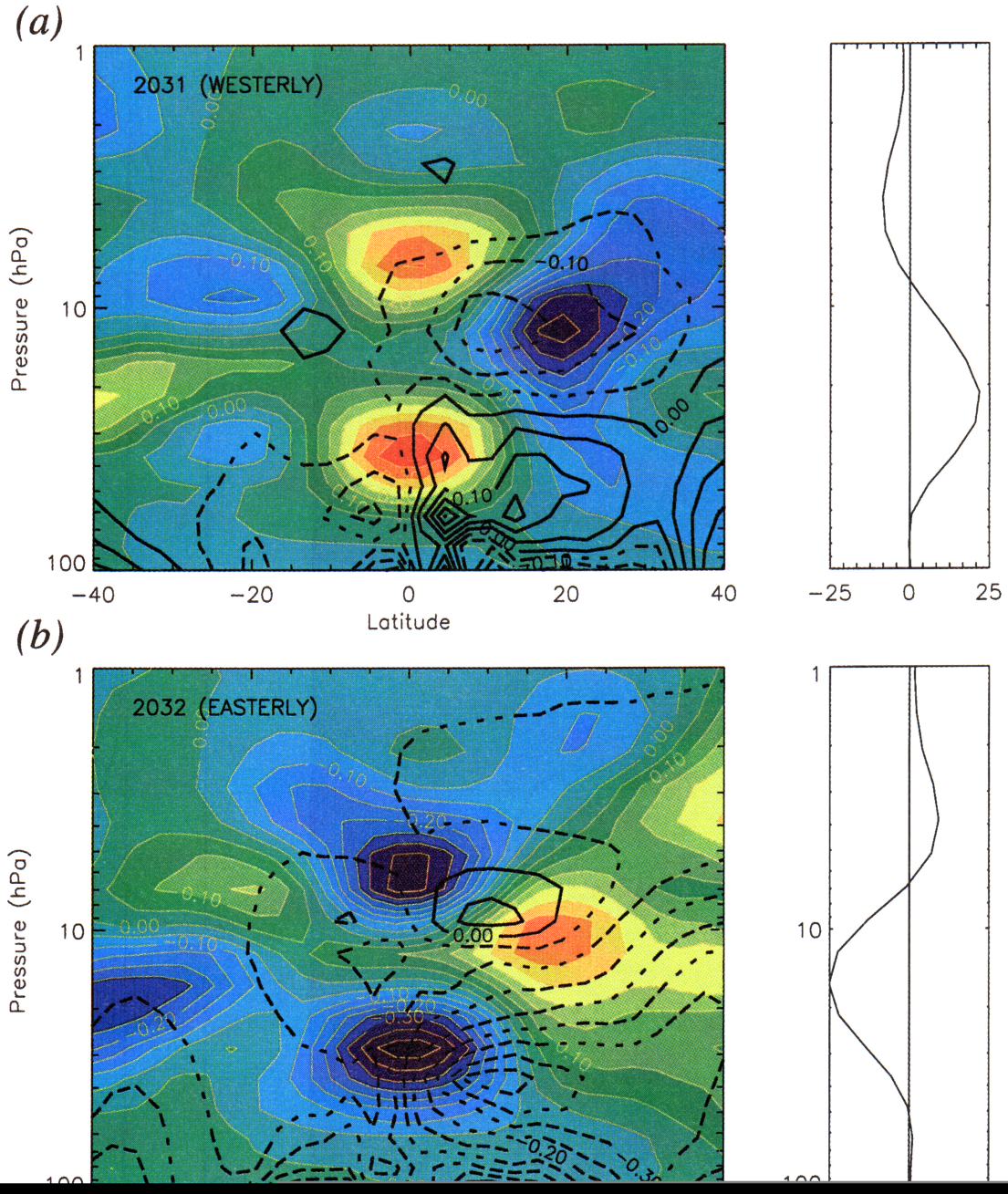
(a)
2031 (WESTERLY)
Pressure (hPa)
1
10
100
−40
−20
0
20
40
Latitude
−25
0
25
(b)
2032 (EASTERLY)
Pressure (hPa)
1
10
100

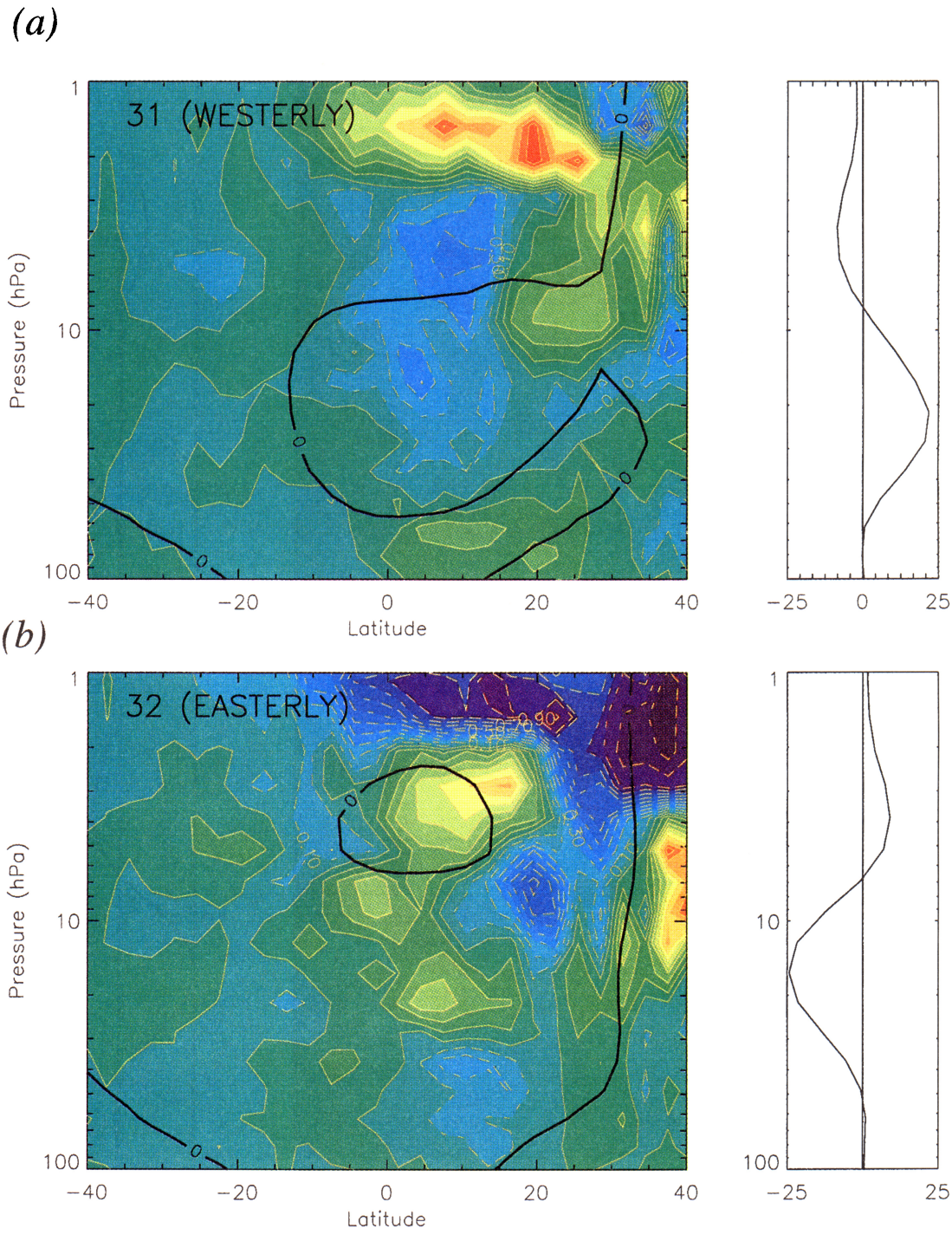

Plate 2. Anomaly ozone eddy transport tendency and the location of the zero wind line for January 31 (westerly) and January 32 (easterly). Units are pptv/s and the contour interval is 0.1 pptv/s.

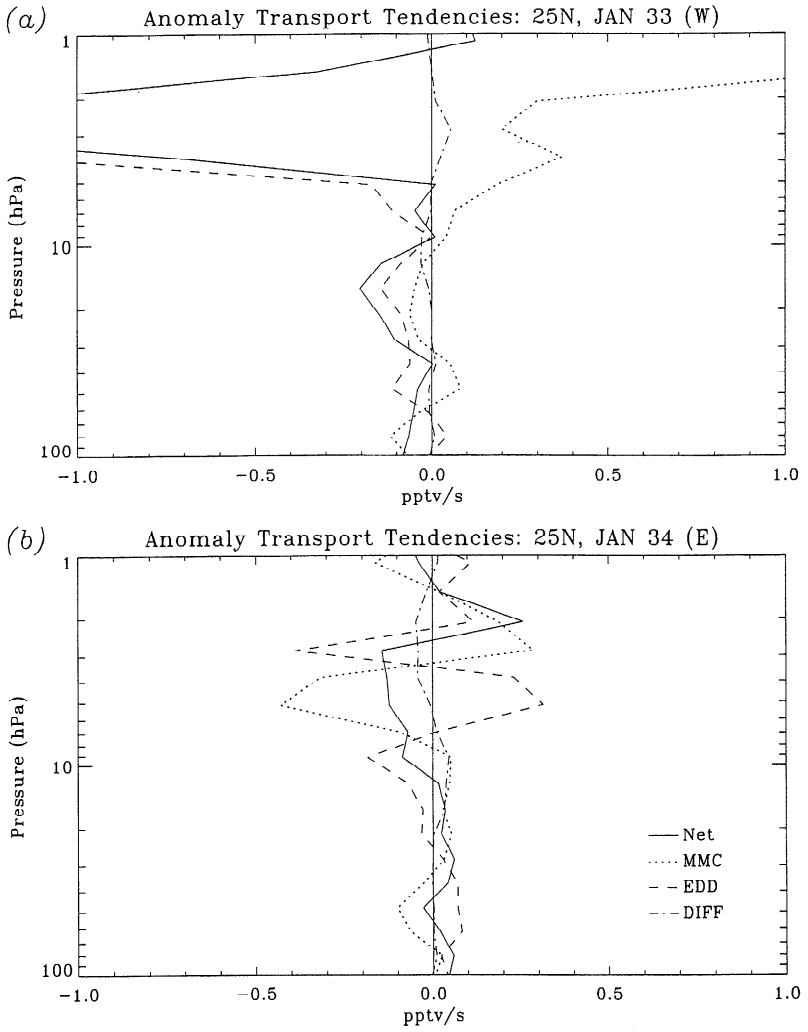

Figure 20. Anomaly ozone transport tendencies at 25°N due to transport by the transformed mean meridional circulation (MMC, dotted line), eddies (EDD, dashed line), and diffusion (DIFF, dashed-dotted line) at the equator for (a) the westerly phase and (b) the easterly phase. Units are in pptv/s. The net transport tendency (NET, solid line) is the sum of the tendencies due to the mean meridional circulation, eddies and diffusion.

primary process driving the ozone QBO in the lower stratosphere, then the maximum easterlies would correspond to a zero in the transport tendency (since the peak easterlies at any level occur roughly when the vertical shear is smallest). The results in Figure 22 indicate that in fact the transport contribution is a quarter-period shifted from this simple expectation, consistent with the results in Figure 21. This is a further indication of the importance of horizontal transport processes in driving the ozone QBO. The net transport tendency at 22.5°N is generally out of phase with the equatorial transport tendency.

Ozone net transport tendency time series near 10 hPa are shown in Figure 23. The negative extremes in equatorial net transport tendency generally occur in association with easterly vertical wind shear (anomalous upwelling), while the positive extremes tend to occur with westerly vertical wind shear (anomalous downwelling). This phase behavior is consistent with what is expected from the vertical advection by the mean circulation. The the net transport tendency at 22.5°N at the 10 hPa level is out of phase with that at the equator.

The total transport tendency may be decomposed into contributions due to the mean meridional circulation and that due to eddies. Each of these terms may be further decomposed into horizontal and vertical components. In principle, this decomposition could be applied to the TEM circulation, but in the present experiment the data necessary to decompose the TEM terms into vertical and horizontal components were not saved. Here the decomposition will be applied to the Eulerian circulation terms, and attention will be restricted to the equator (where Eulerian mean and TEM analysis should produce similar results). Figure 24 shows raw monthly means of the net ozone transport tendency due to the Eulerian mean meridional circulation and due to

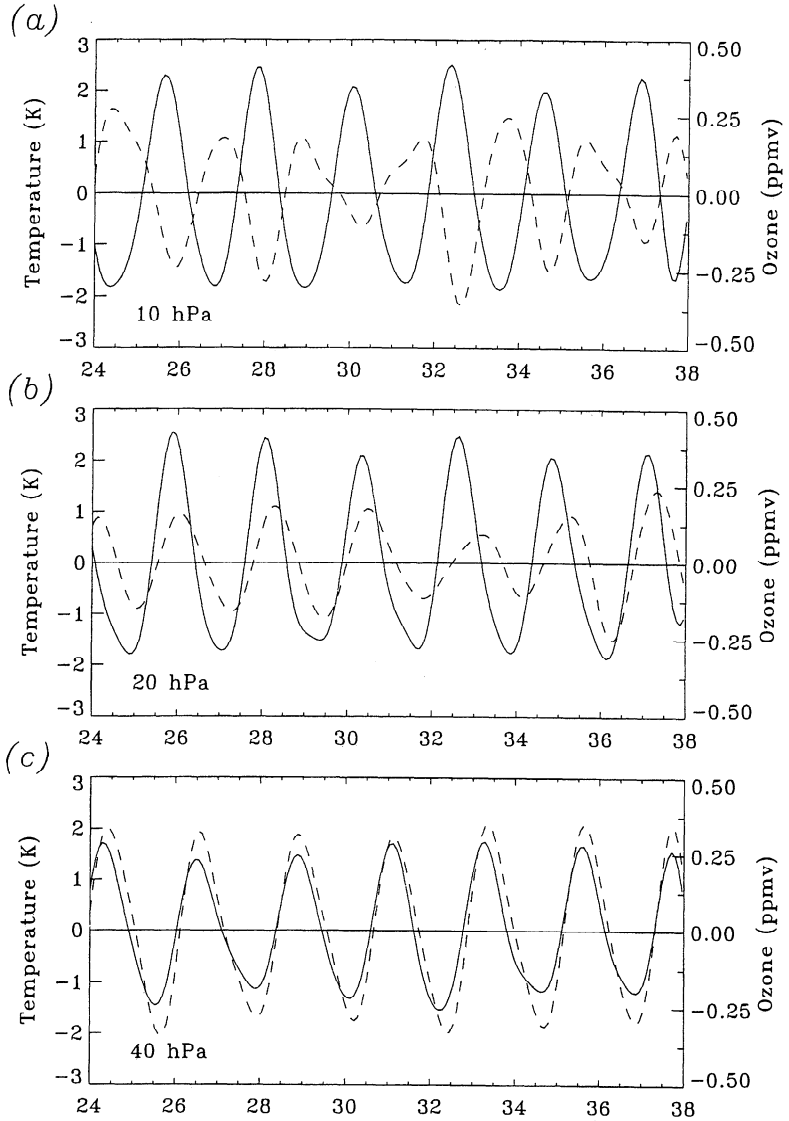

Figure 21. Time series of monthly average ozone (dashed line, right axis) and temperature (solid line, left axis) at selected pressure levels: (a) 10 hPa, (b) 20 hPa, and (c) 40 hPa.

eddies, as well as the horizontal and vertical components of each term, all at the 36.7 hPa level. A time series of the equatorial zonal wind at this level is also shown in the center of Figure 24. The QBO modulation of the transport tendencies is quite apparent.

During years with lower stratospheric easterlies, the eddy transport term (shown in the bottom plot of Figure 24) is rather small, consistent with the expectation that the large planetary waves should be largely excluded from low latitudes. When the mean winds are westerly, however, there is a substantial eddy transport of ozone away from the equator. Transport of ozone by eddies constitutes a significant portion of the total transport tendency at levels down to at least 80 hPa (not shown), although its relative magnitude with respect to the mean meridional transport tendency tends to decrease at lower altitudes. At higher altitudes the eddy transport tendency becomes increasingly important in relation to the mean meridional circulation. It is also interesting that the vertical component of the eddy transport convergence appears to be significantly modulated by the QBO.

Interpretation of the mean meridional circulation transport tendency (top plot in Figure 24) is rather more complicated. Although the vertical component of the transport tendency by the Eulerian mean circulation appears to be consistent with downward (upward) motion associated with westerly (easterly) shear, the results suggest a large degree of cancellation between horizontal and vertical transport (particularly when these transport terms are large). From this, one might conclude that horizontal transport by the Eulerian mean meridional circulation is of comparable importance to vertical transport, in contrast to Reed's original picture of the ozone QBO in which the signal is produced by vertical transport of ozone across a strong vertical con-

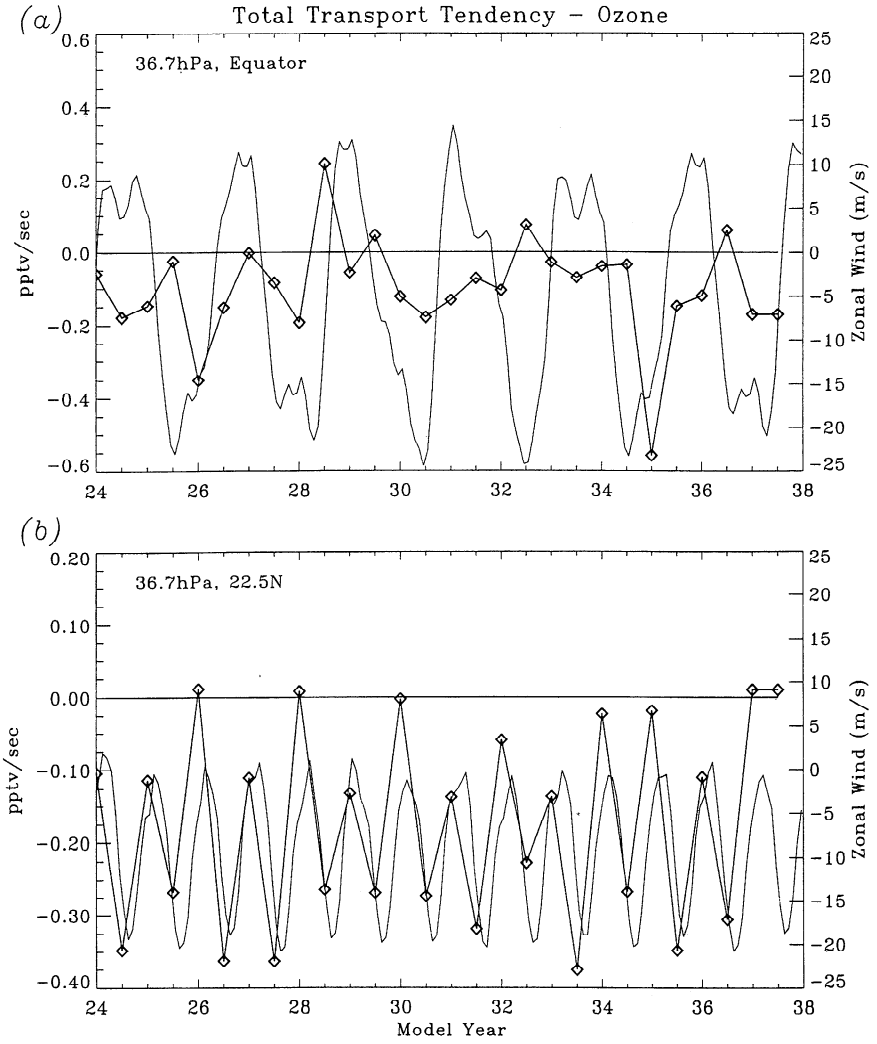

Figure 22. Time series of the total transport tendency of ozone (heavy line, left axis) at 36.7 hPa for (a) the equator and (b) 22.5°N. The light solid line is the unfiltered zonal wind at the same pressure level and latitude. The zonal average transport tendency is available only for the months of January and July, which are indicated by the open symbols on each curve.

centration gradient. The upper plot of Figure 24 may be somewhat misleading, however. The contribution to the ozone mixing ratio from the mean meridional circulation can be written as the negative of the flux divergence

$$\frac{\partial(\omega r)}{\partial p} + \frac{1}{a\cos\theta}\frac{\partial(vr\cos\theta)}{\partial\theta}. \tag{2}$$

But this is equal to

$$r\left(\frac{\partial\omega}{\partial p} + \frac{1}{a\cos\theta}\frac{\partial(v\cos\theta)}{\partial\theta}\right) + \omega\frac{\partial r}{\partial p} + \frac{v}{a}\frac{\partial r}{\partial\theta} \tag{3}$$

where v and ω are the zonal-mean meridional and vertical velocity in pressure coordinates, p is the pressure, r is the ozone mixing ratio, a is the Earth's radius, and θ is latitude. The flux form of equation (2) is the basis for the calculation in the SKYHI model, and (the finite difference representation of) the two terms in (2) are those that are archived (and plotted in Figure 24). The form of equation (3) shows that the negative of the transport term can be written as the sum of the divergence times the local mixing ratio and the product of the velocity with the mixing ratio gradient. The divergence term is zero by continuity, but in general its horizontal and vertical components are nonzero and exactly cancel. In the extreme case of constant mixing ratio, the transport tendency is zero, of course, but there is cancellation between the horizontal and vertical terms when written in flux form. In general, it is reasonable to expect that the use of the flux form to diagnose the vertical and horizontal components of the transport tendency separately could lead to some misleading cancellation of vertical and horizontal terms. Note that the same considerations apply to transport by both the Eulerian and TEM mean meridional circulations.

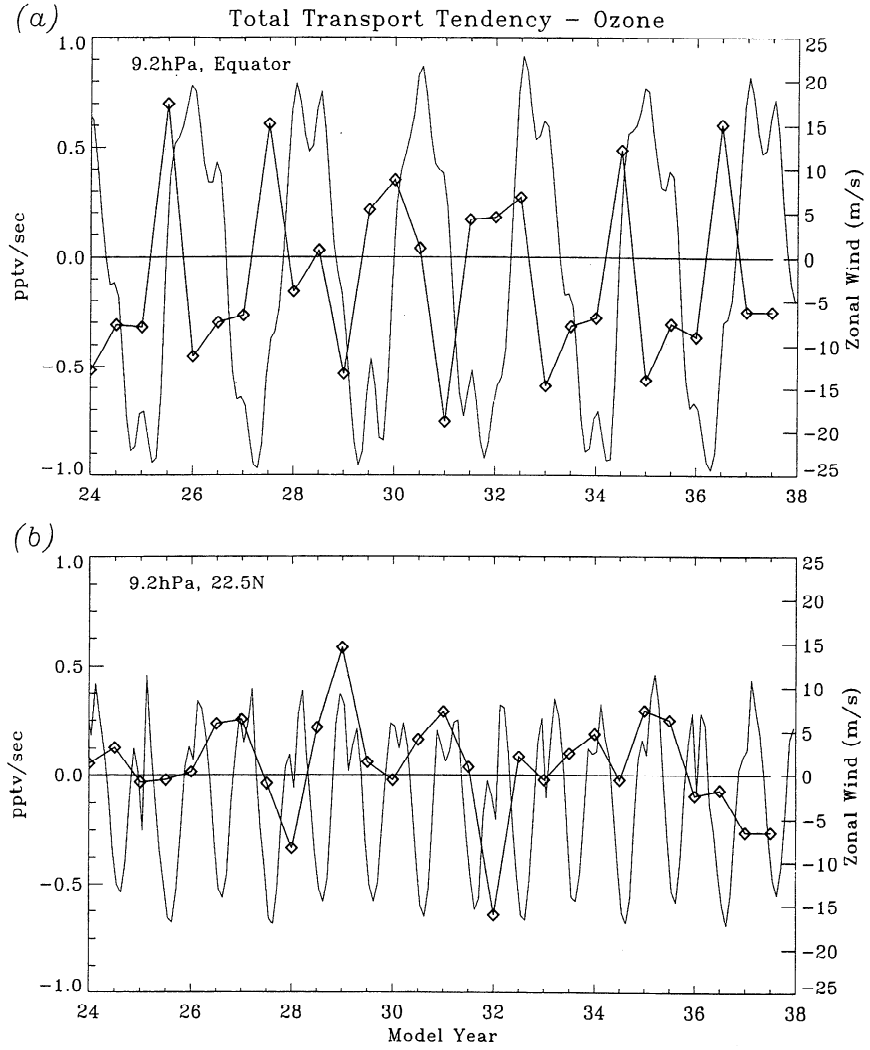

Figure 23. Time series of the total transport tendency of ozone (heavy line, left axis) at 9.2 hPa for (a) the equator and (b) 22.5°N. The light solid line is the unfiltered zonal wind at the same pressure level and latitude. The zonal average transport tendency is available only for the months of January and July, which are indicated by the open symbols on each curve.

Unfortunately, the archived fields from the model do not allow an exact determination of each of last two terms in equation (3). However, using daily means of the zonal-mean wind and ozone mixing ratios, an attempt has been made to estimate these terms for each month (another source of error is introduced because the vertical velocities were not archived on the same level structure that is used by the model in computing vertical derivatives). The upper panel of Figure 25 shows time series of these estimates for the Eulerian mean circulation at the equator and 36.7 hPa. It is clear from this figure that the vertical component of the mean advection dominates the horizontal component by at least a factor of 10. The vertical component also displays a large degree of modulation by the QBO. The lower panel of Figure 25 shows the ozone transport tendencies for the horizontal and vertical components of the TEM circulation estimated in the same way. The Eulerian and TEM transport tendencies are fairly close, and in both the vertical advection dominates the horizontal advection.

As previously noted, the fact that the ozone and temperature QBO signals in the lower stratosphere are approximately in phase suggests that the simple Reed picture of the ozone QBO must be modified. Jones et al. (submitted manuscript, 1999) suggested that the horizontal advection by the mean circulation makes a major contribution. However, their estimates were based on the flux form for the horizontal and vertical terms.

In the present experiment it appears that horizontal transport by the mean meridional circulation is rather unimportant in determining the ozone QBO response, at least in the vicinity of about 40 hPa. Horizontal transport by eddies, however, does play a key role, and this explains why the maximum ozone anomalies at these levels occur nearly in phase with the maximum

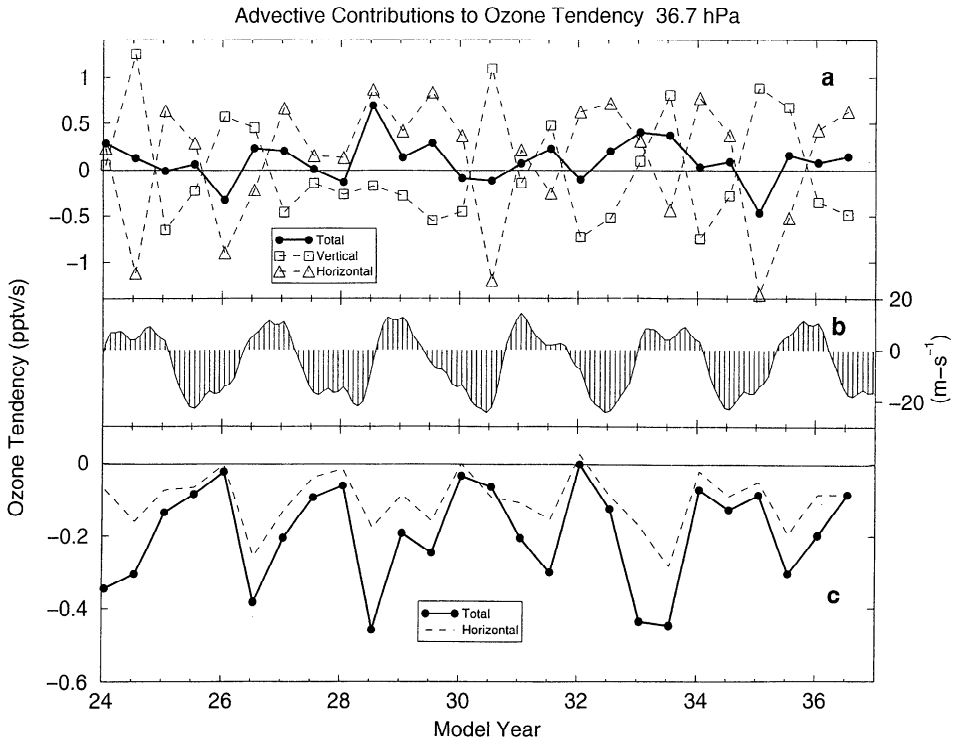

Figure 24. Eulerian mean meridional circulation and eddy contribution to the ozone transport tendency at the equator and 36.7 hPa for each January and July in the experiment (indicated by the open symbols on each curve). The dashed curves give the results obtained for the horizontal and vertical components of the transport, while the heavy solid line represents the net transport tendency. The top plot shows transport tendencies due to the Eulerian mean meridional circulation, the middle plot shows zonal wind at the equator near 40 hPa, and the bottom plot shows eddy transport tendencies. The units are pptv/s for the transport tendencies and m/s for the zonal wind.

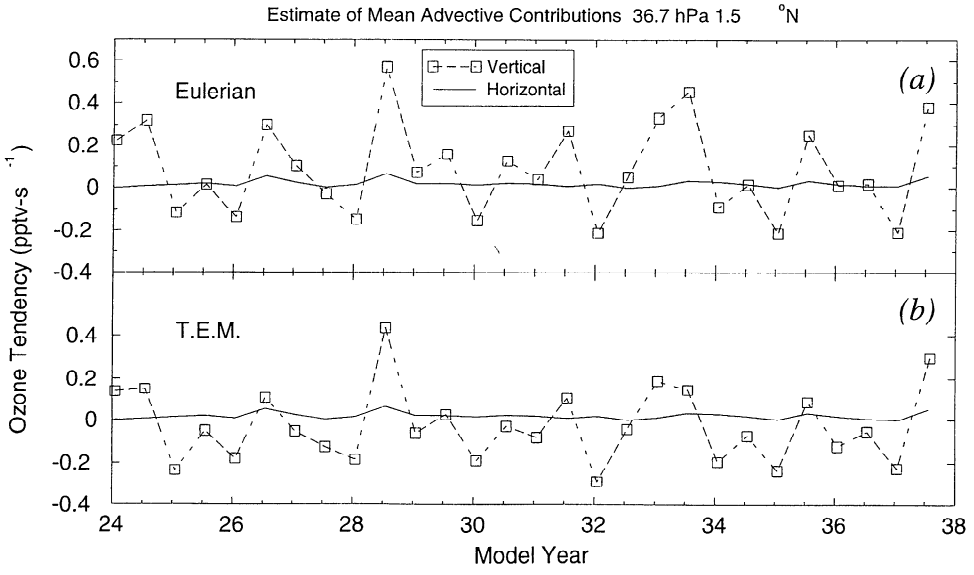

Figure 25. Estimates of ozone transport tendencies due to the Eulerian mean meridional circulation and the transformed-Eulerian mean circulation at the equator and 36.7 hPa for each January and July in the experiment (indicated by the open symbols on each curve). The dashed curve represents the vertical component, while the solid line is the horizontal component. The units are pptv/s.

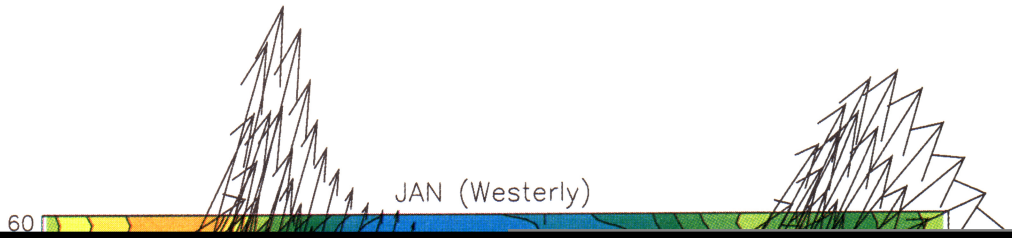
JAN (Westerly)
60

for example in the periodograms of ozone fluctuations at various tropical and subtropical latitudes [*Tung and Yang,* 1994a]. The model does appear to be deficient in not simulating a sufficiently strong ozone QBO in midlatitudes, however.

The simulated vertical structure of the ozone QBO in the tropics and subtropics is also quite realistic. Two areas of maximum QBO amplitude are found in the model simulations of ozone mixing ratio: one centered in the lower stratosphere near 30 hPa, and the other near 8 hPa. The two regions of strong ozone QBO response are separated by a rather abrupt phase reversal near 15 hPa. In agreement with results from earlier studies, it was found that the lower region is due to a quasi-biennial periodicity in ozone transport. The midstratospheric region of ozone QBO response is also ultimately driven by the QBO in circulation, but the effect is indirect. In particular, the QBO in transport modulates the NO_x concentration, and this results in a quasi-biennial signal in the ozone photochemical destruction rate.

When examined in detail, the QBO-induced transport by the transformed-Eulerian mean residual circulation is found to differ significantly from that proposed by *Reed* [1964] in his pioneering work and seen in very idealized models such as that of *Plumb and Bell* [1982]. In particular, the QBO meridional circulation in the present SKYHI simulation was found to be very asymmetric between hemispheres (stronger in the winter) even at very low latitudes. This is in accord with very recent global 2-D model simulations of the QBO circulation that include a full annual cycle [*Jones et al.,* 1998; *Kinnersley and Tung,* 1998; also *Jones et al.,* submitted manuscript, 1999].

In contrast to earlier investigations of this problem, the model used in the present study includes an internally consistent calculation of both eddy and residual mean circulation transport processes. The QBO in the model was shown to systematically modulate the eddy transport tendencies of ozone, at least in the Northern Hemisphere winter. In particular, when there are mean westerlies (easterlies) on the equator, the eddy transport of ozone northward from the equator is significantly enhanced (suppressed). This is consistent with the idea that the QBO modulates the tropical propagation of extratropical planetary waves by shifting the location of the zero wind line [*Holton and Tan,* 1980; *Hamilton,* 1989, 1998a].

The present study has been limited to analysis of model results in the tropics, subtropics, and midlatitudes. There has been some suggestion in the literature that the effects of the equatorial QBO can be detected in high-latitude stratospheric ozone observations of both hemispheres [*Garcia and Solomon,* 1987; *Lait et al.,* 1989; *Butchart and Austin,* 1996], although there is some uncertainty about how significant this effect may be [e.g. *Shuster et al.,* 1989]. As noted in section 2, the present model has severe deficiencies in terms of simulated circulation and temperature in the polar middle atmosphere and so is not appropriate for application to the study of high-latitude ozone. Current development efforts with the SKYHI model are focused on improving the high-latitude circulation (partly through including parameterizations of the effects of subgrid-scale gravity waves), and this may allow future investigations of the role of the QBO in interannual variability of high-latitude ozone.

The present study has demonstrated the usefulness of comprehensive dynamical-chemical GCMs in the study of the interannual variability of the chemical composition of the stratosphere. Future efforts will be devoted to application of the model to other aspects of such variability, notably natural and anthropogenic long-term trends in ozone.

Acknowledgments. The authors thank Jerry Mahlman for his guidance and support during the long model development preliminary to the study discussed here. He has also provided insightful comments on the diagnosis of the results from the QBO experiment. The authors wish to thank Richard Hemler for crucial assistance in implementing the photochemical code within the SKYHI model, and R. John Wilson for his help with aspects of the diagnostic codes. They also thank Hiram Levy, Sam Oltmans, and William Randel for helpful comments on the draft manuscript.

References

Anderson, D.E., Jr., The troposphere-stratosphere radiation field at twilight: A spherical model, *Planet. Space Sci., 31,* 1517-1523, 1983.

Andrews, D.G., and M.E. McIntyre, Planetary waves in horizontal and vertical shear: Asymptotic theory for equatorial waves in a weak shear, *J. Atmos. Sci., 33,* 2031-2048, 1976.

Andrews, D.G., J.R. Holton, and C. Leovy, *Middle Atmosphere Dynamics,* 489 pp., Academic, San Diego, Calif., 1987.

Angell, J.K., and J. Korshover, Quasi-biennial variations in temperature, total ozone and tropopause height, *J. Atmos. Sci., 21,* 479-492, 1964.

Angell, J.K., and J. Korshover, Quasi-biennial and long term fluctuations in total ozone, *Mon. Weather Rev., 101,* 426-443, 1973.

Baldwin, M.R., and K.-K. Tung, Extra-tropical QBO signals in angular momentum and wave forcing, *Geophys. Res. Lett., 21,* 2717-2720, 1994.

Bowman, K.P., Global patterns of the quasi-biennial oscillation in total ozone, *J. Atmos. Sci., 46,* 3328-3343, 1989.

Brasseur, G., and S. Solomon, *Aeronomy of the Middle Atmosphere,* 2nd ed., 452 pp., D. Reidel, Norwell, Mass., 1986.

Butchart, N., and J. Austin, On the relationship between the quasi- biennial oscillation, total chlorine, and the severity of the antarctic ozone hole, *Q. J. R. Meteorol. Soc., 122,* 183-218, 1996.

Chipperfield, M.P., and L.J. Gray, Two-dimensional model studies of the interannual variability of trace gases in the middle atmosphere, *J. Geophys. Res., 97,* 5963-5980, 1992.

Chipperfield, M.P., L.J. Gray, J.S. Kinnersley, and J. Zawodny, A two-dimensional model study of the QBO signal in SAGE II NO_2 and O_3, *Geophys. Res. Lett., 21,* 589-592, 1994.

DeMore, W.D., R.F. Hampson, S.P. Sander, M.J. Kurylo, D.M Golden, C.J. Howard, A.R. Ravishankara, and M.J. Molina, Chemical kinetics and photochemical data for use in stratospheric modeling, *JPL Pub. 90-1,* NASA Jet Propul. Lab., Pasadena, Calif., 1992.

Dunkerton, T.J., The role of gravity waves in the quasi-biennial oscillation, *J. Geophys. Res., 102,* 26,053-26,076, 1997.

Dunkerton, T.J., D.P. Delisi, and M.P. Baldwin, Distribution of major stratospheric sudden warmings in relation to the quasi-biennial oscillation, *Geophys. Res. Lett., 15,* 136-139, 1988.

Fels, S.B., J.D. Mahlman, M.D. Schwarzkopf, and R.W. Sinclair, Stratospheric sensitivity to perturbations in ozone and carbon dioxide: Radiative and dynamical response, *J. Atmos. Sci., 38,* 2265-2297, 1980.

Funk, J.P., and G.L. Garnham, Australian ozone observations and a suggested 24 month cycle, *Tellus, 14,* 378-382, 1962.

Garcia, R.R., and S. Solomon, A numerical model of the zonally averaged dynamical and chemical structure of the middle atmosphere, *J. Geophys. Res., 88,* 1379-1400, 1983.

Garcia, R.R., and S. Solomon, A possible relationship between interannual variability in Antarctic ozone and the quasi-biennial oscillation, *Geophys. Res. Lett., 14,* 848-851, 1987.

Gray, L.J., and T.J. Dunkerton, The role of the seasonal cycle in the quasi-biennial oscillation of ozone, *J. Atmos. Sci., 47,* 2429-2451, 1990.

Gray, L.J., and J.A. Pyle, Two-dimensional model of the quasi-biennial oscillation of ozone, *J. Atmos. Sci., 46,* 203-220, 1989.

Hamilton, K., Interhemispheric asymmetry and annual synchronization of the ozone quasi-biennial oscillation, *J. Atmos. Sci., 46,* 1019-1025, 1989.

Hamilton, K., Interannual variability in the Northern Hemisphere winter middle atmosphere in control and perturbed experiments with the SKYHI general circulation model, *J. Atmos. Sci., 52,* 44-66, 1995a.

Hamilton, K., Comment on "Global QBO in circulation and ozone, Part I: Re-examination of observational evidence", *J. Atmos. Sci., 52,* 1834-1838, 1995b.

Hamilton, K., Comprehensive meteorological modeling of the middle atmosphere: A tutorial review, *J. Atmos. Terr. Phys., 58,* 1591-1628, 1996.

Hamilton, K., Effects of an imposed quasi-biennial oscillation in a comprehensive troposphere-stratosphere-mesosphere general circulation model, *J. Atmos. Sci., 55,* 2392-2418, 1998a.

Hamilton, K., Dynamics of the tropical middle atmosphere: A tutorial review, *Atmos. Ocean, 36,* 319-354, 1998b.

Hamilton, K., R.J. Wilson, J.D. Mahlman, and L.J. Umscheid, Climatology of the GFDL SKYHI troposphere-stratosphere-mesosphere general circulation model, *J. Atmos. Sci., 52,* 5-43, 1995.

Hamilton, K., R.J. Wilson, and R.S. Hemler, The middle atmosphere simulated with high vertical and horizontal resolution versions of a GCM: Improvement in the cold pole bias and generation of a QBO-like oscillation in the tropics, *J. Atmos. Sci.,* in press, 1999.

Hasebe, F., Interannual variations of global total ozone revealed from Nimbus 4 BUV and ground-based observations, *J. Geophys. Res., 88,* 6819-6834, 1983.

Hasebe, F., Quasi-biennial oscillations of ozone and diabatic circulation in the equatorial stratosphere, *J. Atmos. Sci., 51,* 729-745, 1994.

Hilsenrath, E., and B.M. Schlesinger, Total ozone seasonal and interannual variations derived from the 7 year Nimbus-4 BUV dataset, *J. Geophys. Res., 86,* 12,087-12,096, 1981.

Hitchman, M.H., M. McKay, and C.R. Trepte, A climatology of stratospheric aerosol, *J. Geophys. Res., 99,* 20,689-20,700, 1994.

Holton, J.R., Meridional distribution of stratospheric trace constituents, *J. Atmos. Sci., 43,* 1238-1242, 1986.

Holton, J.R., Influence of the annual cycle in meridional transport on the quasi-biennial oscillation in total ozone, *J. Atmos.Sci., 46,* 1434-1439, 1989.

Holton, J.R., and R.S. Lindzen, An updated theory for the quasi-biennial cycle of the tropical stratosphere, *J. Atmos. Sci., 29,* 1076-1080, 1972.

Holton, J.R., and H.-C. Tan, The influence of the equatorial quasi-biennial oscillation on the global circulation at 50 hPa, *J. Atmos. Sci., 37,* 2200-2208, 1980.

Holton, J.R., and H.-C. Tan, The quasi-biennial oscillation in the Northern Hemisphere lower stratosphere, *J. Meteorol. Soc. Jpn., 60,* 140-147, 1982.

Horinouchi, T. and S. Yoden, Wave-mean flow interaction associated with a QBO-like oscillation simulated in a simplified GCM, *J. Atmos. Sci., 55,* 502-526, 1998.

Jones, D.B.A., H.R. Schnieder, and M.B. McElroy, Effects of the quasi-biennial oscillation on the zonally averaged transport of tracers, *J. Geophys. Res., 103,* 11,235-11,250, 1998.

Keating, G., M. Pitts, and D. Young, Ozone reference models for the middle atmosphere, *Adv. Space Res., 10,* 317-355, 1990.

Kinnersley, J.S., Seasonal asymmetry of the low- and middle-latitude QBO circulation anomaly, *J. Atmos. Sci., 56,* 1140-1153, 1999.

Kinnersley, J.S., and K.-K. Tung, Modeling the global interannual variability of ozone due to the equatorial QBO and to extra-tropical planetary wave variability, *J. Atmos. Sci., 55,* 1417-1428, 1998.

Labitzke, K., On the interannual variability of the middle stratosphere during northern winters, *J. Meteorol. Soc. Jpn., 60,* 124-139, 1982.

Lait, L.R., M.R. Schoeberl, and P.A. Newman, Quasi-biennial modulation of the Antarctic ozone depletion, *J. Geophys. Res., 94,* 11,559-11,571, 1989.

Lindzen, R.S., and J.R. Holton, A theory of the quasi-biennial oscillation, *J. Atmos. Sci., 27,* 1095-1107, 1968.

Ling, X.-D., and J. London, The quasi-biennial oscillation of ozone in the tropical middle stratosphere: A one-dimensional model, *J. Atmos. Sci., 43,* 3122-3137, 1986.

Maruyama T., Large-scale disturbances in the equatorial lower stratosphere, *J. Meteorol. Soc. Jpn., 45,* 391-408, 1969.

Minschwaner, K., G.P. Anderson, L.A. Hall, and K. Yoshino, Polynomial coefficients for calculating O_2 Schumann Runge cross sections at 0.5 cm^{-1} resolution, *J. Geophys. Res., 97,* 10,103-10,108, 1992.

Nagashima, T., M. Takahashi, and F. Hasebe, The first simulation of an ozone QBO in a general circulation model, *Geophys. Res. Lett., 25,* 3131-3134, 1998.

Naujokat, B., Update of the observed quasi-biennial oscillation of the stratospheric winds over the tropics, *J. Atmos. Sci., 43,* 1873-1877, 1986.

Oltmans, S.J., and J. London, The quasi-biennial oscillation in atmospheric ozone, *J. Geophys. Res., 87,* 8981-8989, 1982.

O'Sullivan, D., and T.J. Dunkerton, The influence of the quasi-biennial oscillation on global constituent distributions, *J. Geophys. Res., 102,* 21,731-21,743, 1997.

Perliski, L.M., S. Solomon, and J. London, On the interpretation of seasonal variations of stratospheric ozone, *Planet. Space Sci., 37,* 1527-1538, 1989.

Planet, W.G., J.H. Lienesch, A.J. Miller, R. Nagatani, R.D. McPeters, E. Hilsenrath, R.P Cebula, M.T. DeLand, C.G. Wellemayer, and K. Horvath, Northern Hemisphere total ozone values from 1989-1993 determined with the NOAA-11 Solar Backscatter Ultraviolet (SBUV/2) instrument, *Geophys. Res. Lett., 21,* 205-208, 1994.

Plumb, R.A., and R.C. Bell, A model of the quasi-biennial oscillation on an equatorial beta plane, *Q. J. R. Meteorol. Soc., 108,* 335-352, 1982.

Plumb, R.A., and J.D. Mahlman, Zonally averaged transport characteristics of the GFDL general circulation-transport model, *J. Atmos. Sci., 44,* 298-327, 1987.

Politowicz, P.A., and M.H. Hitchman, Exploring the effects of forcing quasi-biennial oscillations in a two-dimensional model, *J. Geophys. Res., 102,* 16,481-16,497, 1997.

Ramanathan, K.R., Bi-annual variation of atmospheric ozone over the tropics, *Q. J. R. Meteorol. Soc., 89,* 540-542, 1963.

Randel, W.J., and F. Wu, Isolation of the ozone QBO in SAGE II data by singular value decomposition, *J. Atmos. Sci., 53,* 2546-2559, 1996.

Randel, W.J., F. Wu, J.M. Russell III, A. Roche, and J.W. Waters, Seasonal cycles and QBO variations in stratospheric CH_4 and H_2O observed in UARS HALOE data, *J. Atmos. Sci., 55,* 163-185, 1998.

Randel, W.J., F. Wu, R. Swinbank, J. Nash, and A. O'Neill, Global QBO circulation derived from UKMO stratospheric analyses, *J. Atmos. Sci., 56,* 457-474, 1999.

Reed, R.J., Evidence for geostrophic motion in the equatorial stratosphere, *Q. J. R. Meteorol. Soc., 88,* 324-327, 1962.

Reed, R.J., A tentative model of the 26-month oscillation in tropical latitudes, *Q. J. R. Meteorol. Soc., 105,* 441-466, 1964.

Reed, R.J., W.J. Campbell, L.A. Rasmussen, and D.G. Rogers, Evidence of a downward-propagating annual wind reversal in the equatorial stratosphere, *J. Geophys. Res., 66,* 813-818, 1961.

Shuster, G.S., R.B. Rood, and M.R. Schoeberl, Quasi-biennial and interannual variability in high resolution total ozone data (TOMS), in *Ozone in the Atmosphere,* edited by R.D. Bojkov and P. Fabian, pp. 260-264, A. Deepak, Hampton, Va., 1989.

Takahashi, M., Simulation of the stratospheric quasi-biennial oscillation using a general circulation model, *Geophys. Res. Lett., 23,* 661-664, 1996.

Tolson, R.H., Spatial and temporal variations of monthly mean total columnar ozone derived from 7 years of BUV data, *J. Geophys. Res., 86,* 7312-7330, 1981.

Tung, K.-K., and H. Yang, Global QBO in circulation and ozone, part I, Re-examination of observational evidence, *J. Atmos. Sci., 51,* 2699-2707, 1994a.

Tung, K.-K., and H. Yang, Global QBO in circulation and ozone, Part II, A simple mechanistic model, *J. Atmos. Sci., 51,* 2708-2721, 1994b.

Veryard, R.G., and R.A. Ebdon, Fluctuations in tropical stratospheric winds, *Meteorol. Mag., 90,* 125-143, 1961.

Zawodny, J.M., and M.P. McCormick, Stratospheric Aerosol and Gas Experiment II measurements of the quasi-biennial oscillations in ozone and nitrogen dioxide, *J. Geophys. Res., 96,* 9371-9377, 1991.

L. Bruhwiler, Climate Monitoring and Diagnostics Laboratory, NOAA/ERL/R/E/CG1, 325 Broadway, Boulder, CO 80303. (e-mail: lbruhwiler@cmdl.noaa.gov)

K. Hamilton, NOAA Geophysical Fluid Dynamics Laboratory, Princeton Forrestal Campus, Route 1, Princeton, NJ 08542. (e-mail: kph@gfdl.gov)

(Received February 12, 1999; revised May 24, 1999; accepted May 27, 1999.)